Uncoupling the Hsp90 and DnaK chaperone activities revealed the *in vivo* relevance of their collaboration in bacteria

Marie Corteggiani[a], Nadège Bossuet-Greif[b], Jean-Philippe Nougayrède[b], Deborah Byrne[c], Marianne Ilbert[a], Sébastien Dementin[a], Marie-Thérèse Giudici-Orticoni[a], Vincent Méjean[a], Eric Oswald[b,d], Olivier Genest[a*]

[a]Aix Marseille Univ, CNRS, BIP UMR 7281, IMM, 31 Chemin Joseph Aiguier, 13402 Marseille, France.

[b]IRSD, INSERM, INRAE, Université de Toulouse, ENVT, Toulouse, France

[c]Protein Expression Facility, Aix Marseille Univ, CNRS, IMM, 31 Chemin Joseph Aiguier, 13402 Marseille, France.

[d]CHU Toulouse, Hôpital Purpan, Service de Bactériologie-Hygiène, Toulouse, France

[*]Correspondence: Olivier Genest, CNRS, Aix Marseille Univ, BIP UMR 7281, 31 Chemin Joseph Aiguier, 13402 Marseille, Cedex 20, France.

Email: ogenest@imm.cnrs.fr

Phone: +33 4 91 16 46 53

Classification: Biological Sciences/Microbiology

Keywords: HtpG; Hsp70; heat stress; proteostasis; colibactin

Running title: *In vivo* Hsp90-DnaK collaboration

Abstract

Chaperone proteins are essential in all living cells to ensure protein homeostasis. Hsp90 is a major ATP-dependent chaperone highly conserved from bacteria to eukaryotes. Recent studies have shown that bacterial Hsp90 is essential in some bacteria in stress conditions, and that it participates in the virulence of pathogenic bacteria. *In vitro*, bacterial Hsp90 directly interacts and collaborates with the Hsp70 chaperone DnaK to reactivate model substrate proteins, however it is still unknown whether this collaboration is relevant *in vivo* with physiological substrates. Here, we used site-directed mutagenesis on Hsp90 to impair DnaK binding, thereby uncoupling the chaperone activities. We tested the mutants *in vivo* in two bacterial models in which Hsp90 has known physiological functions. We found that the Hsp90 point mutants were defective to support (i) growth under heat stress and activation of an essential Hsp90 client in the aquatic bacterium *Shewanella oneidensis*, and (ii) biosynthesis of the colibactin toxin involved in the virulence of pathogenic *Escherichia coli*. Our study therefore demonstrates the essentiality of the direct collaboration between Hsp90 and DnaK *in vivo* in bacteria to support client folding. It also suggests that this collaboration already functional in bacteria has served as an evolutionary basis for a more complex Hsp70-Hsp90 collaboration found in eukaryotes.

Significance

Protein homeostasis is controlled in every cell by a class of proteins called chaperones. Hsp90 and Hsp70 are two chaperones that are conserved from bacteria to human. In this article, we demonstrate that *in vivo* in bacteria, the physiological activity of the Hsp90 chaperone requires a direct binding and collaboration with DnaK, the bacterial Hsp70 chaperone. This was highlighted by working with two bacterial models on different pathways including the biosynthesis of a toxin involved in bacterial virulence. Our study suggests that this bacterial chaperone collaboration has served as an evolutionary basis to give rise to more complex eukaryotic chaperone systems.

Introduction

Protein folding in the cell is a crucial process that is complicated by non-optimal physico-chemical conditions, including temperature shifts or crowding of intracellular macromolecules. To ensure protein homeostasis - also called proteostasis - under normal and stress conditions, every living cells possess a complex network of molecular chaperones and proteases (1–4). The ATP-dependent chaperone Hsp90 (Heat shock protein of 90 kDa) is highly conserved from bacteria to eukaryotes (5–11). Hsp90 is essential in eukaryotes and hundreds of substrate proteins, called clients, have been identified. Among its clients, Hsp90 allows the folding of oncoproteins in cancer cells; therefore, many molecules blocking the activity of Hsp90 have been developed (12, 13). In bacteria, although few clients are known, Hsp90 (also called HtpG) has been shown to be essential under stress in some genus including the aquatic model bacterium *Shewanella oneidensis* and the cyanobacterium *Synechococcus elongatus* (11, 14–20). In addition, Hsp90 participates by still unknown mechanisms in the virulence of pathogenic bacteria like extraintestinal pathogenic *Escherichia coli* (ExPEC), *Salmonella* Typhimurium or *Pseudomonas aeruginosa* (21–25).

Hsp90 is a dimeric protein composed of three domains: an N-terminal domain that binds nucleotides, a middle domain where most clients interact, and a C-terminal domain possessing the dimerization interface. To function, the Hsp90 dimer cycles between several conformations (5, 26, 27). In the absence of nucleotide, Hsp90 is predominantly in an open V-shape conformation, with dimerization only occurring via the C-terminal domains of the two protomers. Client and ATP binding favor Hsp90 dimer closure with additional contacts between the N-terminal domains of the two protomers (28–30). After ATP hydrolysis, client and ADP are released and Hsp90

returns to the open conformation. Hsp90 co-chaperones, which are found only in eukaryotes, also modulate the structural dynamics of Hsp90.

Hsp90 is known to function in concert with the Hsp70 chaperone, although in bacteria the physiological relevance of this collaboration is still unknown (6, 31). Hsp70 (called DnaK in bacteria) is a highly conserved ATP-dependent chaperone that contains a nucleotide binding domain connected by a flexible linker to a substrate binding domain (32, 33). DnaK/Hsp70 cycles between two main conformations controlled by the presence of ATP or ADP in the nucleotide binding domain, leading respectively to the opening or the closure of the substrate binding domain. The cycle of DnaK/Hsp70 is regulated by two cochaperones, a J-domain protein (including DnaJ/Hsp40) that targets substrates to DnaK/Hsp70 and stimulates ATP hydrolysis, and a protein from the Nucleotide Exchange Factor (NEF) family that triggers ADP release from DnaK/Hsp70 (34, 35). DnaK/Hsp70 interacts with hydrophobic sequences present in most proteins. In addition to the activity of DnaK/Hsp70, some protein substrates require the activity of the Hsp90 chaperone, and therefore the chaperone cycles of Hsp70/DnaK and Hsp90 are interconnected (6, 11, 31, 36).

The bacterial Hsp90 and DnaK proteins provide an interesting simple model system to study the collaboration between the two chaperones, in part due to the absence of Hsp90 cochaperones in bacteria (37–42). In the collaboration model drawn from *in vitro* experiments from several groups using model substrates, the DnaK chaperone assisted by a J-domain cochaperone first interacts with the denatured substrate and partially remodels it (Fig. 1A). Then, through a direct interaction between the two chaperones, the substrate is transferred to Hsp90 to achieve client remodeling. The regions of interaction between Hsp90 and DnaK have been identified in *E. coli* proteins:

they include regions from the middle domain of Hsp90 and from the nucleotide binding domain of DnaK (37, 39, 40).

Although the mechanism of action of the *in vitro* collaboration between bacterial Hsp90 and the DnaK system is getting clearer, a crucial point is to know whether this model mostly drawn from *in vitro* experiments is physiologically relevant in bacteria. Taking advantage of the knowledge on the interaction between Hsp90 and DnaK, we uncoupled the activities of both chaperones by site-directed mutagenesis on Hsp90. We then tested the ability of the mutants to sustain known functions of Hsp90 in two bacterial models, *Shewanella oneidensis* in which Hsp90 is essential for growth under heat stress, and *E. coli* in which Hsp90 is required for the biosynthesis of a genotoxin involved in virulence and colon carcinogenesis (15, 22). Our experiments demonstrate that to function *in vivo*, Hsp90 requires the collaboration and the direct interaction with DnaK.

Results

Identification of $Hsp90_{So}$ mutants affected for DnaK binding *in vivo*.

Here, our goal was to assess whether the collaboration and direct interaction between Hsp90 and DnaK is needed for the known functions of Hsp90 *in vivo*. To address this point, we used the aquatic bacterium *Shewanella oneidensis* since we have found that Hsp90 ($Hsp90_{So}$) is required for its growth under heat stress (15). We have previously identified a region in the middle domain of Hsp90 from *E. coli* ($Hsp90_{Ec}$) that is involved in DnaK binding, and mutation of key residues in this region strongly decreased the interaction with DnaK (39). $Hsp90_{So}$ and $Hsp90_{Ec}$ are highly conserved; their amino acid sequences share 69 % identity and more than 80 % similarity. We mutated

residues of $Hsp90_{So}$ that are homologous to the $Hsp90_{Ec}$ residues known to be involved in the interaction with DnaK (Fig. 1B and C, Fig. S1). The residues we mutated are all in the middle domain of Hsp90: K247 ($Hsp90_{So}$ numbering) is located in a loop at the N-terminal extremity of the middle domain, the two residues G279 and K280 are also in a loop that connects two β-sheets, and the residue R364 is found in the largest helix from the middle domain (Fig. 1B and D). These residues are all on the surface of Hsp90 and are in close vicinity (Fig. 1D). Therefore, testing Hsp90 mutants affected for DnaK binding in *S. oneidensis* is a good way to evaluate the importance of the Hsp90-DnaK collaboration *in vivo*.

To show that the residues we mutated in $Hsp90_{So}$ indeed prevent DnaK binding, we first used a bacterial two-hybrid method. It has been shown that this method is suitable to measure *in vivo* the interaction between bacterial Hsp90 and DnaK (38, 39). $Hsp90_{So}$ wild-type or mutant and DnaK from *S. oneidensis*, $DnaK_{So}$, were fused to one subdomain (T25 or T18) of the catalytic domain of the adenylate cyclase of *Bordetella pertussis*. If $Hsp90_{So}$ and $DnaK_{So}$ interact, the T25 and T18 subdomains become close enough to reconstitute the catalytic domain of the adenylate cyclase, leading to cAMP production, and indirectly to the production of β-galactosidase, whose activity was measured (43, 44). As expected, we observed a significant interaction between $Hsp90_{So}$ and $DnaK_{So}$ (Fig. 2A), as already shown with the proteins from *E. coli* (38, 39). When we measured the interaction with the mutant proteins, we found that the interaction between $DnaK_{So}$ and $Hsp90_{So}$(K247C) or $Hsp90_{So}$(G279A-K280A) was decreased by about 50 %, while the mutation R364C reduced the interaction to less than 30 % compared to the wild-type protein (Fig. 2A). To further impact the interaction, we combined the mutations G279A-K280A and R364C. Importantly, substitutions of these three residues strongly reduced the interaction with $DnaK_{So}$, with a level of β-

galactosidase activity of about 15 % compared to wild-type. As a control, we showed that the mutant proteins were produced at the same level as wild-type Hsp90$_{So}$, and that the mutations we selected did not affect the ability of Hsp90$_{So}$ to dimerize (Fig. S2 A and B).

Co-purifications between DnaK$_{So}$ and Hsp90$_{So}$ wild-type or mutants were performed to confirm the results obtained by the bacterial two-hybrid experiments. DnaK$_{So}$ with a 6His tag, and Hsp90$_{So}$ wild-type or mutants with a CBP tag were produced in *E. coli*. Cells were lysed and Hsp90$_{So}$ wild-type and mutants were purified on calmodulin beads. Proteins were separated on SDS-PAGE and Western blot analysis indicated whether DnaK$_{So}$ co-purified or not with Hsp90$_{So}$. As expected, we found that Hsp90$_{So}$ wild-type interacted with DnaK$_{So}$ (Fig. 2B and Fig. S3). However, the Hsp90$_{So}$(R364C) and Hsp90$_{So}$(G279A-K280A-R364C) mutants very weakly co-purified with DnaK$_{So}$ (Fig. 2B and Fig. S3). We confirmed that Hsp90$_{So}$ wild-type and mutants, as well as DnaK$_{So}$, were produced at the same level before co-purification (Fig. 2B, input panels). These experiments confirm that the mutations in Hsp90 strongly diminished binding with DnaK.

The Hsp90$_{So}$ mutants as well as the wild-type proteins were purified and ITC experiments were performed to test their direct binding with DnaK$_{So}$ *in vitro*. A weak interaction between Hsp90$_{So}$ and DnaK$_{So}$ was measured with a K_D~21 µM (Fig. S4A and F), in accordance with previous results obtained with DnaK/Hsp70 and Hsp90 chaperones from *E. coli*, yeast, or the endoplasmic reticulum (40, 45, 46). In these experimental conditions, we did not measure any interaction with the mutants Hsp90$_{So}$(R364C) and Hsp90$_{So}$(G279A-K280A-R364C) (Fig. S4B and C).

We next characterized the Hsp90$_{So}$ mutants to confirm that the mutations we selected only affect DnaK$_{So}$ binding, and no other function of the protein. We found that the

mutants behaved similarly to wild-type on size exclusion chromatography (Fig. S2C) and with circular dichroism experiments (Fig. S2D and E). We also found that the mutations did not affect $Hsp90_{So}$ ATPase activity (Fig. S5A, gray bars). Additional experiments using the $Hsp90_{Ec}$ client protein L2 suggest that the mutations did not impact client binding nor conformational changes induced by the client. Indeed, L2 has been shown to interact with $Hsp90_{Ec}$ and to stimulate its ATPase activity (47). Interestingly, we observed that L2 similarly stimulated the ATPase activity of $Hsp90_{So}$ wild-type and mutants (Fig. S5A, blue bars). Another client, TilS from *S. oneidensis*, was also tested for binding with $Hsp90_{So}$ wild-type and mutants. When heterologously overproduced from plasmids in *E. coli*, $Hsp90_{So}$(R364C) and $Hsp90_{So}$(G279A-K280A-R364C) co-purified with TilS similarly to $Hsp90_{So}$ wild-type, whereas mutations in the main client binding region of $Hsp90_{So}$, W476R-L563A, impaired TilS binding (Fig. S5B and C) (15). Finally, purified $Hsp90_{So}$(G279A-K280A-R364C) prevented TilS aggregation as observed with wild-type $Hsp90_{So}$ (Fig. S5D) (15), reinforcing the idea that the Hsp90 mutants defective for DnaK binding are not impaired for client binding.

Altogether, we identified several mutations in $Hsp90_{So}$ that strongly reduce the interaction with $DnaK_{So}$ without impacting Hsp90 global folding, ATPase activity, client binding, nor conformational changes associated with client binding. Therefore, the activity of the two chaperones can be uncoupled to analyze the impact of Hsp90 acting independently of DnaK.

Hsp90 mutants impaired for DnaK binding do not support bacterial growth under heat stress.

We have previously found that a *S. oneidensis* Δ*hsp90*$_{So}$ strain grew very poorly under heat stress (35°C) although it grew as the wild-type strain at permissive temperature (28°C) (15). To test whether the Hsp90$_{So}$ mutants can rescue the growth of the Δ*hsp90*$_{So}$ strain under heat stress, plasmids coding for Hsp90$_{So}$ wild-type or mutants (K247C, G279A-K280A, R364C, and G279A-K280A-R364C) under the control of an inducible promoter were introduced in the Δ*hsp90*$_{So}$ strain, and the resulting strains were grown on plates in the presence of the arabinose inducer at 28°C and 35°C (Fig. 3A and S6A). At 35°C, Hsp90$_{So}$ wild-type and the two Hsp90$_{So}$ mutants (K247C and G279A-K280A) that showed the weakest decrease in DnaK$_{So}$ binding fully rescued the growth of the Δ*hsp90*$_{So}$ strain (Fig. 3A). In contrast, the Hsp90$_{So}$ mutants with the strongest defects in DnaK$_{So}$ binding partially (R364C) or barely (G279A-K280A-R364C) support growth of the Δ*hsp90*$_{So}$ strain. Similar phenotypes were observed when the strains were grown in liquid cultures under heat stress (Fig. 3B). As expected, no difference in growth was observed at 28°C between the strains producing Hsp90$_{So}$ wild-type or mutants on plates and in liquid cultures (Fig. S6A and B).

To further demonstrate the importance of the interaction between DnaK and Hsp90 in physiological conditions, the mutations R364C and G279A-K280A-R364C were introduced in the chromosome of *S. oneidensis* at the *hsp90*$_{So}$ locus, leading to the strains noted here as *hsp90*$_{So}$(R364C) and *hsp90*$_{So}$(G279A-K280A-R364C), respectively. Although the mutation R364C partially affected *S. oneidensis* growth under heat stress, the triple mutation G279A-K280A-R364C led to a similar drastic growth defect as observed with the Δ*hsp90*$_{So}$ strain at 35°C both on plates and in liquid cultures, whereas the wild-type strain grew well (Fig. 3C and D). At 28°C, the four strains grew similarly (Fig. S6C and D). Western blot analysis showed that

Hsp90$_{So}$(R364C) and Hsp90$_{So}$(G279A-K280A-R364C) produced from plasmids or from the chromosome were as abundant as wild-type Hsp90$_{So}$ (Fig. S6E and F).

Altogether, these experiments strongly suggest that the function of Hsp90$_{So}$ under heat stress requires the direct interaction and collaboration with DnaK$_{So}$. To further study the functional interaction between the two chaperones, we also mutated DnaK residues known to be important for Hsp90 binding (Supporting Results, Fig. S7 and S8) (40). We showed by two-hybrid and co-purification experiments that the DnaK$_{So}$(E216A-V217A) mutant had reduced binding with Hsp90$_{So}$ (Fig. S7C and E). When these mutations were introduced in the chromosome of *S. oneidensis* at the *dnaK$_{So}$* locus, growth of *S. oneidensis* was reduced under heat stress, giving weight to our model of collaboration *in vivo* (Fig. S8C and E). However, since Hsp90 and DnaJ share binding regions on DnaK (40, 48, 49), the results obtained with the DnaK mutants might also result from a decrease in DnaJ binding.

The direct interaction between Hsp90 and DnaK is needed for TilS activation and protection.

In a previous study, we have identified a client of Hsp90 in *S. oneidensis*, TilS, whose activation and protection depend on the activity of Hsp90 under heat stress (15). However, it remained to be known whether the collaboration between Hsp90$_{So}$ and DnaK$_{So}$ was required or not for these activities. TilS is an essential enzyme in bacteria allowing the maturation of a tRNA that is absolutely needed for the translation of the AUA codon into isoleucine (50, 51). The activity of TilS can be measured *in vivo* by using a genetic construction on a plasmid, called p(AUA)*lacZ*, in which a DNA sequence containing 4 ATA codons was inserted between the initiator codon (ATG)

and the coding sequence of *lacZ*, the gene encoding the β-galactosidase enzyme (15, 52). Therefore, with this construct, the translation and the activity of the β-galactosidase depend on the activity of TilS (Fig. 4A).

The p(AUA)*lacZ* plasmid as well as a control plasmid without the ATA sequences upstream of *lacZ*, p*lacZ*, were introduced into *S. oneidensis* wild-type, Δ*hsp90*$_{So}$, *hsp90*$_{So}$(R364C) or *hsp90*$_{So}$(G279A-K280A-R364C). Strains were grown either at permissive temperature (28°C) or at sub-lethal temperature (34°C), expression of the *lacZ* reporter gene was induced, and we measured β-galactosidase activity. At 28°C, a similar level of β-galactosidase activity was observed in the strains containing the p(AUA)*lacZ* plasmid, indicating as expected that, at this temperature, the activity of TilS was not affected by the absence of Hsp90$_{So}$ and therefore by the Hsp90 mutations (Fig. S9A) (15). In contrast, at sub-lethal temperature (34°C), the level of β-galactosidase activity was reduced about 3 times in the Δ*hsp90*$_{So}$ strain compared to the wild-type, as previously shown since Hsp90$_{So}$ is required at this temperature for TilS remodeling (Fig. 4B) (15). Interestingly, a similar 3-time decrease was measured in the strain producing the mutant Hsp90$_{So}$(G279A-K280A-R364C) that showed the strongest defect in DnaK$_{So}$ binding, while the Hsp90$_{So}$(R364C) mutant only led to a slight decrease in β-galactosidase activity (Fig. 4B). The activity of TilS was also reduced (about 2 times) in the presence of the DnaK$_{So}$(E216A-V217A) mutant affected for Hsp90$_{So}$ binding (Fig. S8G). To confirm that the decrease in β-galactosidase activity observed above did not result from a general defect in protein production in the absence of Hsp90$_{So}$, or with the Hsp90$_{So}$ or DnaK$_{So}$ mutants, experiments were performed with the p*lacZ* control plasmid. A similar level of β-galactosidase activity was measured under heat stress in the different strains (Fig. 4B and S8G), clearly

showing that the defects observed with the p(AUA)*lacZ* plasmid depend on the translation of the AUA codons, and therefore on the activity of TilS.

In the absence of Hsp90$_{So}$, TilS is degraded by the HslVU protease (15, 53). Using the Hsp90$_{So}$ mutants, we wondered whether the protection of TilS by Hsp90$_{So}$ necessitates the collaboration with DnaK$_{So}$. To test that, a plasmid allowing the production of TilS with a 6His tag was introduced in *S. oneidensis* wild-type, the Δ*hsp90$_{So}$* strain, or in the two strains bearing the Hsp90 mutations on the chromosome, *hsp90$_{So}$*(R364C) and *hsp90$_{So}$*(G279A-K280A-R364C). After growth and induction of the expression of TilS, cells were collected, proteins were separated on SDS-PAGE, transferred on Western blots and detected using an anti-6His antibody. We observed that the intensity of the band corresponding to TilS was strongly reduced in the Δ*hsp90$_{So}$* strain compared to the wild-type (Fig. 4C and D) (15, 53). Although a similar level of the band corresponding to TilS was observed in the strain producing the Hsp90$_{So}$(R364C) mutant, degradation occurred in the strain producing Hsp90$_{So}$(G279A-K280A-R364C) that has a strong defect in binding DnaK$_{So}$ (Fig. 4C and D). At 28°C, no significant degradation was observed in the absence of Hsp90$_{So}$ or with the mutants as expected, since Hsp90$_{So}$ is not needed to protect TilS at permissive temperature (Fig. S9B) (15, 53).

Taken together, these results demonstrate that the activation and protection of TilS require the direct interaction and the collaboration between Hsp90 and DnaK.

The direct collaboration between Hsp90 and DnaK is essential for the biosynthesis of colibactin in *E. coli.*

To extend the essential nature of the interaction and collaboration between Hsp90 and DnaK to the *in vivo* physiological activities of Hsp90, we used a known phenotype of the absence of Hsp90 in *E. coli*. Indeed, it has been shown that Hsp90 (noted here as $Hsp90_{Ec}$) is involved in the biosynthesis of colibactin, a genotoxic toxin that leads to DNA damage in eukaryotic cells (54). Colibactin belongs to the family of hybrid polyketide/nonribosomal peptide (PK-NRP). It is synthesized by a large NRP-PK synthetase machinery, encoded by a 54-kb gene cluster, the *pks* genomic island (54, 55). Although the direct target of Hsp90 in this biosynthetic pathway is not known, it has been shown that *pks+ E. coli* strains devoid of $Hsp90_{Ec}$ does not produce colibactin (22).

To evaluate the importance of the interaction between DnaK from *E. coli* ($DnaK_{Ec}$) and $Hsp90_{Ec}$ in the production of colibactin, we used the wild-type *E. coli* strain M1/5 that possesses the *pks* island (22). Plasmids coding for $Hsp90_{Ec}$ wild-type or mutants including $Hsp90_{Ec}$(R355C) which have been shown to no longer interact with $DnaK_{Ec}$ (39) were introduced in the M1/5 strain deleted of the $hsp90_{Ec}$ gene (Fig. 1C). Then, colibactin production was measured by quantifying the phosphorylation of histone H2AX in response to DNA damage in HeLa cells exposed to each *E. coli* strains (22) (Fig. 5A). We verified that the various mutations in $Hsp90_{Ec}$ did not affect *E. coli* growth during the interaction with the HeLa cells and that the mutants were produced at the same level as the wild-type protein (Fig. S10A and S10B). As previously published, the absence of $Hsp90_{Ec}$ dramatically reduced the production of colibactin, and this production was restored by Hsp90 wild-type (Fig. 5B). The mutants $Hsp90_{Ec}$(K238C) and $Hsp90_{Ec}$(G270A-K271A) exhibited a partial (~70 %) restoration whereas $Hsp90_{Ec}$(R355C) and $Hsp90_{Ec}$(G270A-K271A-R355C) barely or did not restore

colibactin production, respectively (Fig. 5B). Therefore, collaboration between Hsp90 and DnaK is also essential in *E. coli* to allow colibactin production.

Discussion

For years, the physiological importance of the bacterial Hsp90 chaperone has been underestimated since its absence only modestly impacts *E. coli* growth in laboratory conditions (56). Nowadays, we know that bacterial Hsp90 is essential in some environmental bacteria and that it plays crucial roles in other bacteria where it is involved in unanticipated pathways including for example the CRISPR system or the biosynthesis of complex molecules such as toxins and siderophores (15, 19, 20, 22). Its role in the virulence of several pathogenic bacteria has also been documented (21–25). In parallel, many biochemical studies have been performed to characterize the *in vitro* chaperone activity of *E. coli* Hsp90 ($Hsp90_{Ec}$) (38, 39, 41, 57). Experiments using denatured model substrates including luciferase revealed that purified *E. coli* Hsp90 was unable to remodel alone the substrate, it actually required the presence of the DnaK chaperone and its two cochaperones (38, 41). Notably, bacterial Hsp90 and DnaK directly interact and the regions of interaction between the two chaperones have been defined: they include residues from the middle domain of Hsp90, and residues from the nucleotide binding domain of DnaK, which is also the region important for DnaJ binding (37, 39, 40, 48, 49). However, the *in vivo* physiological relevance of the collaboration between Hsp90 and DnaK had never been demonstrated in bacteria.

Therefore, given the vast knowledge acquired on the *in vitro* mechanism of action of bacterial Hsp90 and recent findings about its physiological functions, we wondered whether the collaboration between Hsp90 and DnaK is crucial for Hsp90 functions *in*

vivo as shown *in vitro* with model substrates. We uncoupled the chaperone activities of Hsp90 and DnaK by site-directed mutagenesis on Hsp90, allowing the two chaperones to conserve their activities independently of each other. The Hsp90 mutants we obtained were tested using two model organisms, the aquatic bacteria *S. oneidensis* and an *E. coli* commensal strain that synthesizes the genotoxin colibactin as in extra-intestinal pathogenic *E. coli*. Our results show that *in vivo*, direct contacts between the two chaperones are required to allow an efficient collaboration between DnaK and Hsp90, and in particular client folding by Hsp90. Indeed, when the interaction between the two chaperones was impaired by point mutations, Hsp90 was unable (i) to support growth under heat stress (Fig. 3) and to allow TilS activation and protection in *S. oneidensis* (Fig. 4), and (ii) to promote colibactin biosynthesis in *E. coli* (Fig. 5). We also uncoupled the chaperone activities of Hsp90 and DnaK by site-directed mutagenesis on DnaK (Fig. S7). Mutations in the Hsp90-binding region of DnaK also led to reduced growth of *S. oneidensis* under heat stress, and reduced TilS activity (Fig. S8). These results therefore strengthen the model of an *in vivo* direct collaboration between Hsp90 and DnaK. However, given the overlap between this region and the one involved in DnaJ binding, the results with the DnaK mutants appeared difficult to interpret and the defects observed could also result from issues in DnaK-DnaJ functional interaction (Supporting Results, Fig. S7 and S8) (37, 40, 48, 49).

Altogether, our data imply that the Hsp90 clients must be directly transferred from DnaK to Hsp90, and instead cannot be released in the cytosol after DnaK remodeling to later be taken in charge by Hsp90. The clients might be in unstable conformations that have to be maintained by DnaK before being directly transferred to Hsp90. In agreement with this hypothesis, it has been proposed that the DnaK/Hsp70 chaperone

inhibits the folding process of some clients including the glucocorticoid receptor and the tumor suppressor protein p53, and this inhibition is relieved by Hsp90, reinforcing the necessity of a direct transfer of the client between the two chaperones (36, 41, 58, 59). Alternatively, in mammalian cells, some clients could also be transferred to Hsp90 without direct Hsp70-Hsp90 contact as it has been shown recently with the NudC co-chaperone that facilitates the transfer of the glucocorticoid receptor and p53 directly from Hsp40 to Hsp90 (60).

We have previously observed that TilS is degraded by the HslVU protease in the absence of $Hsp90_{So}$ (53). Here, our results provide insights into the mechanism of the degradation. Indeed, we found that TilS is degraded when the interaction between DnaK and $Hsp90_{So}$ is strongly impaired (Fig. 4C), implying that the action of DnaK alone does not lead to a protease-resistant conformation of TilS. These results reinforce the hypothesis of a competition between Hsp90 and HslVU to bind TilS (53). However, the direct transfer of TilS from DnaK to Hsp90 could limit the possibility of degradation by HslVU. Interestingly, experiments suggest that the HslVU protease is responsible of the degradation of the Hsp90 clients involved in colibactin biosynthesis, even if these clients have not been identified yet (22). Therefore, as previously proposed, an intricate network of chaperones and proteases could finely control the level of some proteins involved in important processes such as tRNA maturation or toxin biosynthesis (22, 53, 61). The tight regulation of the balance between folding by the Hsp70/Hsp90 chaperones and degradation by the proteasome has also been documented in eukaryotes with an unexpected involvement of the Hsp90 cochaperone HOP that, in addition to facilitate binding between Hsp90 and Hsp70, also allows proteasome activation (62).

A model of the collaboration between Hsp90 and DnaK in bacteria has emerged from *in vitro* work (6, 11, 37–42), and our study now demonstrates the physiological relevance of this model. An unfolded substrate is recognized by a J-domain protein (DnaJ for example) and is transferred to the ATP-bound conformation of DnaK. After ATP hydrolysis, ADP-bound DnaK tightly interacts with the substrate. Release of the substrate is then facilitated by the cochaperone GrpE and several rounds of substrate binding and release eventually lead to substrate folding. For some substrates (Hsp90 clients), the action of the DnaK system is not sufficient, and Hsp90 is required to achieve folding, activation or to allow quaternary structure assembly. In that case, DnaK bound to a client interacts with the middle domain of Hsp90, and this interaction is stabilized by the J-domain protein and the client. The client is transferred to Hsp90, and ATP binding and hydrolysis lead to closure of the Hsp90 dimer, allowing client protection and folding. An additional layer of complexity is provided *in vivo* by the interplay between chaperones, proteases, and possibly other still unknown actors of the proteostasis network.

Evolutionary analyses on chaperone proteins indicate that Hsp70 and Hsp90 have first emerged in bacteria before being acquired by eukaryotes (63). Interestingly, Hsp90 is found only in organisms that also possess Hsp70, although the opposite is not true, suggesting that some Hsp70 substrates require an upgraded chaperone activity provided by Hsp90. Our study reinforces this hypothesis by showing that the collaboration between Hsp90 and DnaK is paramount in bacteria. The ancestral Hsp90-DnaK machine has then evolved with the appearance of many Hsp90 cochaperones in eukaryotes to face and adapt to the higher complexity of the proteome. Nonetheless, we also analyzed the conservation of the amino acid residues involved in the interaction between Hsp90 and Hsp70/DnaK mutated in this study.

Although the residues G279-K280 ($Hsp90_{So}$ numbering) are not strictly conserved in Hsp90 proteins, it is noteworthy to point out that the residue R364 is either conserved in $Hsp90_{Ec}$ and Trap1, or substituted by another positively charged amino acid, a lysine in yeast Hsp82, and human Hsp90α and Grp94 (Fig. S1). This residue has first been identified in *E. coli* Hsp90 (residue R355) in a genetic screen looking for mutations that prevent DnaK binding (39). Interestingly, mutation of the equivalent residue in the endoplasmic reticulum Hsp90, Grp94 (K467) (46), in yeast Hsp82 (K399) (45), or in cytosolic human Hsp90α (K419) (62) disrupts the binding with Hsp70. This positively charged residue could form a salt bridge with a conserved glutamic acid residue in Hsp70/DnaK as observed in a recent cryo-electron microscopy structure from the Agard lab (Fig. S11) (36). Mutation of this glutamic acid residue in $DnaK_{So}$ (E216) (Fig. S7), in $DnaK_{Ec}$ (E217) (40), and in the Hsp70 endoplasmic reticulum protein BiP (E243) (46) reduces binding between Hsp90 and Hsp70.

In this study, we demonstrate the physiological importance of the direct interaction between bacterial Hsp90 and DnaK, and in particular for the production of a genotoxin involved in the virulence of extra-intestinal pathogenic *E. coli*. Interestingly, it is known that Hsp90 participates in the virulence of several pathogenic bacteria (21–25). Since multidrug resistant bacteria now represent a huge public health issue, it becomes crucial to develop alternative strategies to limit the virulence of these bacteria. One possibility would be to block Hsp90 activity using the large amount of already known inhibitors of eukaryotic Hsp90 that could be optimized to specifically be targeted to bacterial Hsp90. Alternatively, our study opens up the possibility of developing molecules that would decrease binding between DnaK and Hsp90, therefore limiting bacterial virulence.

Materials and methods

Strains, plasmids, and growth conditions. Strains used in this study are listed in Table S1. The wild-type *S. oneidensis* strain is MR1-R (64), and the wild-type commensal *E. coli* strain used for colibactin production is M1/5 (65). The *S. oneidensis* Δ*hsp90*$_{So}$ and *E. coli* Δ*hsp90*$_{Ec}$ strains deleted of their respective *htpG* genes have been constructed previously (15, 22). The *S. oneidensis* strains *hsp90*$_{So}$(R364C) and *hsp90*$_{So}$(G279A-K280A-R364C) carry chromosomal mutations in the *htpG* gene; they were constructed as described in Supporting Materials and Methods.

Plasmids used in this study are listed in Table S2. Plasmid construction is described in Supporting Materials and Methods. Site-directed mutagenesis experiments were performed using the QuickChange mutagenesis kit (Agilent) by using the manufacturer's instructions. Mutations were checked by sequencing. Plasmids were introduced by conjugation in *S. oneidensis* strains and by transformation in *E. coli* strains.

Strains were grown aerobically in LB rich medium with shaking at the temperatures indicated. When necessary, ampicillin (50 µg/mL), kanamycin (50 µg/mL), chloramphenicol (25 µg/mL) or streptomycin (100 µg/mL) was added.

Bacterial two-hybrid assays. Bacterial two-hybrid assays were performed as previously described with some modifications (43). Bth101Δ*htpG E. coli* strain lacking the adenylate cyclase gene was co-transformed with two plasmids, one coding for the T18 domain of the adenylate cyclase from *Bordetella pertussis* fused to the DnaK protein from *S. oneidensis* (pT18-dnaK$_{So}$), and the other coding for the T25 domain of the adenylate cyclase from *B. pertussis* fused to the Hsp90 wild-type or mutant protein from *S. oneidensis* (pT25-hsp90$_{So}$ WT or mutant). As negative controls, vectors

producing the T18 (pUT18-C-linker) or T25 (pKT25-linker) domains alone were used. Transformants were incubated two days at 28°C. Colonies were inoculated in rich LB medium supplemented with kanamycin, ampicillin, and 1mM IPTG. After overnight incubation at 28°C, cells were lysed with PopCulture Reagent solution (Agilent) and 1 mg/mL lysozyme during 15 min, before addition of Z buffer (100 mM phosphate buffer pH = 7, 10mM KCl, 1 mM $MgSO_4$, 50mM β-mercaptoethanol). 2.2 mM ortho-nitrophényl-β-galactoside (ONPG) was added and β-galactosidase activity was measured using a modified Miller assay adapted for use in a Tecan Spark microplate reader as described previously (66).

Co-purification assays. Interaction of $Hsp90_{So}$ wild-type or mutants with $DnaK_{So}$ was performed by co-purification assays using calmodulin beads as previously described (15). Briefly, *E. coli* MG1655*Δhsp90*$_{Ec}$ strains containing the plasmids pCBP-*hsp90*$_{So}$ wild-type or mutants, and p*dnaK*$_{So}$-6His were grown at 37°C to OD_{600}=0.8. As negative controls, plasmids pBad33-CBP and pBad24 were used. Then, 0.05 % arabinose was added to allow production of CBP-$Hsp90_{So}$ and $DnaK_{So}$-6His for 1 h. Cells were collected, lysed by French Press in CBP buffer (150 mM Tris HCl pH=8, 150 mM NaCl, 1 mM Mg acetate, 1 mM imidazole, 2 mM $CaCl_2$, 0.1 % Triton, 10 mM β-mercaptoethanol), centrifuged, and the supernatant was incubated for 1 h with 50 µL CBP affinity resin (Agilent). After 4 washes with CBP buffer, the resin was resuspended in 40 µL loading buffer, and was heat-denatured at 95°C for 10 min. Purified protein samples and protein extracts before purification (input) were loaded on SDS-PAGE and transferred by Western Blot. $Hsp90_{So}$ was detected with an anti-$Hsp90_{Ec}$ antibody (57) and $DnaK_{So}$ with an anti-His antibody (Thermo). Co-purifications between TilS and $Hsp90_{So}$ were performed as described (15).

Effects of Hsp90$_{So}$ mutants on *S. oneidensis* growth. These experiments were performed as previously with some modifications (15). After overnight precultures at 28°C in LB medium, the *S. oneidensis* strains without plasmids or with plasmids derived from pBad33 were inoculated to OD_{600} = 0.1 in LB with antibiotics when necessary, and incubated at 28°C until late exponential phase. For growth on solid media, cells were diluted to OD_{600}=1, and 3 µL of 10-time serial dilutions were spotted on LB-agar plates supplemented with 0.01 % arabinose where indicated. Plates were incubated at 28°C overnight, and at 35°C for 24 h. For growth in liquid media, cells were diluted to OD_{600}= 0.0005 in LB supplemented with 0.015 % arabinose when necessary. Growth was measured in a microplate reader at 28°C or 38°C.

Reporter assays to follow TilS activity *in vivo*. TilS activity was followed by *in vivo* reporter assay in the *S. oneidensis* wild-type, *Δhsp90$_{So}$*, *hsp90$_{So}$*(R364C) and *hsp90$_{So}$*(G279A-K280A-R364C) strains containing p(AUA)*lacZ* or p*lacZ* plasmids as previously described (15). Strains were grown at 28°C overnight with chloramphenicol. Cells diluted to OD_{600}=0.1 were incubated at 28°C or 34°C, and three hours later, 0.2 % arabinose was added. After 2 hours, β-galactosidase activity was measured using a modified Miller assay adapted for use in a Tecan Spark microplate reader as described previously (66).

Western blot analysis to evaluate TilS amount. TilS amount was determined by Western blots as previously described (15). The p*lacZ-tilS$_{6His}$* plasmid was introduced into the wild-type, *Δhsp90$_{So}$*, *hsp90$_{So}$*(R364C) and *hsp90$_{So}$*(G279A-K280A-R364C) *S. oneidensis* strains. These strains were grown at 28°C overnight with chloramphenicol,

diluted to OD_{600} = 0.1 and incubated at 28°C or 34°C for 3 hours. 0.02 % arabinose was added, and 2 hours later, the same amount of cells was collected. Pellets were resuspended in denaturing loading buffer, heat treated at 95°C, and proteins were separated by SDS-PAGE and transferred by Western blot. TilS was detected with a anti-6His antibody (Thermo). AtcJ protein of *S. oneidensis* was detected with anti-AtcJ antibody as neutral loading control (66).

Effects of $Hsp90_{Ec}$ mutants on production of the genotoxin colibactin by *E. coli*. Production of colibactin by *E. coli* strain M1/5 was determined as previously described (22). Briefly, after overnight growth in LB, bacteria were pre-cultivated 2 hours in interaction medium (DMEM Hepes, Sigma, supplemented with 0.02 % arabinose) and human epithelial HeLa cells were exposed in the interaction medium during 4 h to the live *E. coli* strains with an initial dose of 200 bacteria per cell. Bacterial growth was recorded by measuring OD_{600}, the HeLa cells were washed and further incubated 4 h with gentamicin. The HeLa cells were then fixed and the phosphorylation of histone H2AX in response to colibactin-induced DNA damage was quantified by in-cell western, using anti-p-H2AX antibodies and infrared fluorescent secondary antibodies, with a plate reader (Licor). The genotoxicity was normalized to the DNA-fluorescent stain and indexed to the background level in control cells (22). The assay was repeated three times.

Statistical analysis

All statistical analyses were performed with GraphPad Prism software (version 8) using one-way ANOVA with Tukey's multiple comparisons test assuming Gaussian distribution of residuals and equal SDs. Summary of results were shown as significant

(****: p-value ≤ 0.0001; ***: p-value ≤ 0.001; **: p-value ≤ 0.01; *: p-value ≤ 0.05) or not significant (ns: p-value > 0.05)

Acknowledgements

We thank members of our groups for help and fruitful discussions. This work was supported by the Centre National de la Recherche Scientifique, Aix Marseille Université, INSERM, INRAE, ENVT, Université Paul Sabatier, and the Agence Nationale de la Recherche (ANR-20-CE44-0017).

References

1. D. Balchin, M. Hayer-Hartl, F. U. Hartl, In vivo aspects of protein folding and quality control. *Science* **353**, aac4354 (2016).

2. V. Dahiya, J. Buchner, Functional principles and regulation of molecular chaperones. *Adv. Protein Chem. Struct. Biol.* **114**, 1–60 (2019).

3. A. Finka, R. U. H. Mattoo, P. Goloubinoff, Experimental Milestones in the Discovery of Molecular Chaperones as Polypeptide Unfolding Enzymes. *Annu. Rev. Biochem.* **85**, 715–742 (2016).

4. M. S. Hipp, P. Kasturi, F. U. Hartl, The proteostasis network and its decline in ageing. *Nat. Rev. Mol. Cell Biol.* **20**, 421–435 (2019).

5. M. M. Biebl, J. Buchner, Structure, Function, and Regulation of the Hsp90 Machinery. *Cold Spring Harb. Perspect. Biol.* **11** (2019).

6. O. Genest, S. Wickner, S. M. Doyle, Hsp90 and Hsp70 chaperones: Collaborators in protein remodeling. *J. Biol. Chem.* **294**, 2109–2120 (2019).

7. J. L. Johnson, Evolution and function of diverse Hsp90 homologs and cochaperone proteins. *Biochim. Biophys. Acta* **1823**, 607–613 (2012).

8. M. Radli, S. G. D. Rüdiger, Dancing with the Diva: Hsp90-Client Interactions. *J. Mol. Biol.* **430**, 3029–3040 (2018).

9. F. H. Schopf, M. M. Biebl, J. Buchner, The HSP90 chaperone machinery. *Nat. Rev. Mol. Cell Biol.* **18**, 345–360 (2017).

10. M. Taipale, D. F. Jarosz, S. Lindquist, HSP90 at the hub of protein homeostasis: emerging mechanistic insights. *Nat. Rev. Mol. Cell Biol.* **11**, 515–528 (2010).

11. S. Wickner, T.-L. L. Nguyen, O. Genest, The Bacterial Hsp90 Chaperone: Cellular Functions and Mechanism of Action. *Annu. Rev. Microbiol.* **75**, 719–739 (2021).

12. L. M. Butler, R. Ferraldeschi, H. K. Armstrong, M. M. Centenera, P. Workman, Maximizing the Therapeutic Potential of HSP90 Inhibitors. *Mol. Cancer Res. MCR* **13**, 1445–1451 (2015).

13. Y. Miyata, H. Nakamoto, L. Neckers, The therapeutic target Hsp90 and cancer hallmarks. *Curr. Pharm. Des.* **19**, 347–365 (2013).

14. J. Buchner, Bacterial Hsp90--desperately seeking clients. *Mol. Microbiol.* **76**, 540–544 (2010).

15. F. A. Honoré, V. Méjean, O. Genest, Hsp90 Is Essential under Heat Stress in the Bacterium Shewanella oneidensis. *Cell Rep.* **19**, 680–687 (2017).

16. M. M. Hossain, H. Nakamoto, HtpG plays a role in cold acclimation in cyanobacteria. *Curr. Microbiol.* **44**, 291–296 (2002).

17. M. M. Hossain, H. Nakamoto, Role for the cyanobacterial HtpG in protection from oxidative stress. *Curr. Microbiol.* **46**, 70–76 (2003).

18. T. Sato, S. Minagawa, E. Kojima, N. Okamoto, H. Nakamoto, HtpG, the prokaryotic homologue of Hsp90, stabilizes a phycobilisome protein in the cyanobacterium Synechococcus elongatus PCC 7942. *Mol. Microbiol.* **76**, 576–589 (2010).

19. N. Tanaka, H. Nakamoto, HtpG is essential for the thermal stress management in cyanobacteria. *FEBS Lett.* **458**, 117–123 (1999).

20. I. Yosef, M. G. Goren, R. Kiro, R. Edgar, U. Qimron, High-temperature protein G is essential for activity of the Escherichia coli clustered regularly interspaced short palindromic repeats (CRISPR)/Cas system. *Proc. Natl. Acad. Sci. U. S. A.* **108**, 20136–20141 (2011).

21. W. Dang, Y. Hu, L. Sun, HtpG is involved in the pathogenesis of Edwardsiella tarda. *Vet. Microbiol.* **152**, 394–400 (2011).

22. C. Garcie, *et al.*, The Bacterial Stress-Responsive Hsp90 Chaperone (HtpG) Is Required for the Production of the Genotoxin Colibactin and the Siderophore Yersiniabactin in Escherichia coli. *J. Infect. Dis.* **214**, 916–924 (2016).

23. A. M. Grudniak, B. Klecha, K. I. Wolska, Effects of null mutation of the heat-shock gene htpG on the production of virulence factors by Pseudomonas aeruginosa. *Future Microbiol.* **13**, 69–80 (2018).

24. E. Verbrugghe, *et al.*, HtpG contributes to Salmonella Typhimurium intestinal persistence in pigs. *Vet. Res.* **46**, 118 (2015).

25. T. Dong, *et al.*, Involvement of the Heat Shock Protein HtpG of Salmonella Typhimurium in Infection and Proliferation in Hosts. *Front. Cell. Infect. Microbiol.* **11**, 758898 (2021).

26. K. A. Krukenberg, T. O. Street, L. A. Lavery, D. A. Agard, Conformational dynamics of the molecular chaperone Hsp90. *Q. Rev. Biophys.* **44**, 229–255 (2011).

27. M. P. Mayer, Gymnastics of molecular chaperones. *Mol. Cell* **39**, 321–331 (2010).

28. M. M. U. Ali, *et al.*, Crystal structure of an Hsp90-nucleotide-p23/Sba1 closed chaperone complex. *Nature* **440**, 1013–1017 (2006).

29. A. K. Shiau, S. F. Harris, D. R. Southworth, D. A. Agard, Structural Analysis of E. coli hsp90 reveals dramatic nucleotide-dependent conformational rearrangements. *Cell* **127**, 329–340 (2006).

30. D. R. Southworth, D. A. Agard, Species-dependent ensembles of conserved conformational states define the Hsp90 chaperone ATPase cycle. *Mol. Cell* **32**, 631–640 (2008).

31. T. Morán Luengo, M. P. Mayer, S. G. D. Rüdiger, The Hsp70-Hsp90 Chaperone Cascade in Protein Folding. *Trends Cell Biol.* **29**, 164–177 (2019).

32. M. P. Mayer, L. M. Gierasch, Recent advances in the structural and mechanistic aspects of Hsp70 molecular chaperones. *J. Biol. Chem.* **294**, 2085–2097 (2019).

33. R. Rosenzweig, N. B. Nillegoda, M. P. Mayer, B. Bukau, The Hsp70 chaperone network. *Nat. Rev. Mol. Cell Biol.* **20**, 665–680 (2019).

34. P. Genevaux, C. Georgopoulos, W. L. Kelley, The Hsp70 chaperone machines of Escherichia coli: a paradigm for the repartition of chaperone functions. *Mol. Microbiol.* **66**, 840–857 (2007).

35. E. A. Craig, J. Marszalek, How Do J-Proteins Get Hsp70 to Do So Many Different Things? *Trends Biochem. Sci.* **42**, 355–368 (2017).

36. R. Y.-R. Wang, *et al.*, Structure of Hsp90-Hsp70-Hop-GR reveals the Hsp90 client-loading mechanism. *Nature* **601**, 460–464 (2022).

37. S. M. Doyle, *et al.*, Intermolecular Interactions between Hsp90 and Hsp70. *J. Mol. Biol.* **431**, 2729–2746 (2019).

38. O. Genest, J. R. Hoskins, J. L. Camberg, S. M. Doyle, S. Wickner, Heat shock protein 90 from Escherichia coli collaborates with the DnaK chaperone system in client protein remodeling. *Proc. Natl. Acad. Sci. U. S. A.* **108**, 8206–8211 (2011).

39. O. Genest, J. R. Hoskins, A. N. Kravats, S. M. Doyle, S. Wickner, Hsp70 and Hsp90 of E. coli Directly Interact for Collaboration in Protein Remodeling. *J. Mol. Biol.* **427**, 3877–3889 (2015).

40. A. N. Kravats, *et al.*, Interaction of E. coli Hsp90 with DnaK Involves the DnaJ Binding Region of DnaK. *J. Mol. Biol.* **429**, 858–872 (2017).

41. T. Morán Luengo, R. Kityk, M. P. Mayer, S. G. D. Rüdiger, Hsp90 Breaks the Deadlock of the Hsp70 Chaperone System. *Mol. Cell* **70**, 545–552.e9 (2018).

42. H. Nakamoto, *et al.*, Physical interaction between bacterial heat shock protein (Hsp) 90 and Hsp70 chaperones mediates their cooperative action to refold denatured proteins. *J. Biol. Chem.* **289**, 6110–6119 (2014).

43. A. Battesti, E. Bouveret, The bacterial two-hybrid system based on adenylate cyclase reconstitution in Escherichia coli. *Methods San Diego Calif* **58**, 325–334 (2012).

44. G. Karimova, J. Pidoux, A. Ullmann, D. Ladant, A bacterial two-hybrid system based on a reconstituted signal transduction pathway. *Proc. Natl. Acad. Sci.* **95**, 5752–5756 (1998).

45. A. N. Kravats, *et al.*, Functional and physical interaction between yeast Hsp90 and Hsp70. *Proc. Natl. Acad. Sci. U. S. A.* **115**, E2210–E2219 (2018).

46. M. Sun, J. L. M. Kotler, S. Liu, T. O. Street, The endoplasmic reticulum (ER) chaperones BiP and Grp94 selectively associate when BiP is in the ADP conformation. *J. Biol. Chem.* **294**, 6387–6396 (2019).

47. Y. Motojima-Miyazaki, M. Yoshida, F. Motojima, Ribosomal protein L2 associates with E. coli HtpG and activates its ATPase activity. *Biochem. Biophys. Res. Commun.* **400**, 241–245 (2010).

48. R. Kityk, J. Kopp, M. P. Mayer, Molecular Mechanism of J-Domain-Triggered ATP Hydrolysis by Hsp70 Chaperones. *Mol. Cell* **69**, 227–237.e4 (2018).

49. C. S. Gässler, *et al.*, Mutations in the DnaK chaperone affecting interaction with the DnaJ cochaperone. *Proc. Natl. Acad. Sci. U. S. A.* **95**, 15229–15234 (1998).

50. K. Nakanishi, *et al.*, Structural basis for translational fidelity ensured by transfer RNA lysidine synthetase. *Nature* **461**, 1144–1148 (2009).

51. T. Suzuki, K. Miyauchi, Discovery and characterization of tRNAIle lysidine synthetase (TilS). *FEBS Lett.* **584**, 272–277 (2010).

52. A. Soma, *et al.*, An RNA-modifying enzyme that governs both the codon and amino acid specificities of isoleucine tRNA. *Mol. Cell* **12**, 689–698 (2003).

53. F. A. Honoré, N. J. Maillot, V. Méjean, O. Genest, Interplay between the Hsp90 Chaperone and the HslVU Protease To Regulate the Level of an Essential Protein in Shewanella oneidensis. *mBio* **10**, e00269-19 (2019).

54. J.-P. Nougayrède, *et al.*, Escherichia coli induces DNA double-strand breaks in eukaryotic cells. *Science* **313**, 848–851 (2006).

55. C. V. Chagneau, *et al.*, The pks island: a bacterial Swiss army knife?: Colibactin: beyond DNA damage and cancer. *Trends Microbiol.*, S0966-842X(22)00122–6 (2022).

56. J. C. Bardwell, E. A. Craig, Ancient heat shock gene is dispensable. *J. Bacteriol.* **170**, 2977–2983 (1988).

57. O. Genest, *et al.*, Uncovering a region of heat shock protein 90 important for client binding in E. coli and chaperone function in yeast. *Mol. Cell* **49**, 464–473 (2013).

58. V. Dahiya, *et al.*, Coordinated Conformational Processing of the Tumor Suppressor Protein p53 by the Hsp70 and Hsp90 Chaperone Machineries. *Mol. Cell* **74**, 816–830.e7 (2019).

59. M. Boysen, R. Kityk, M. P. Mayer, Hsp70- and Hsp90-Mediated Regulation of the Conformation of p53 DNA Binding Domain and p53 Cancer Variants. *Mol. Cell* **74**, 831–843.e4 (2019).

60. M. M. Biebl, *et al.*, NudC guides client transfer between the Hsp40/70 and Hsp90 chaperone systems. *Mol. Cell* **82**, 555–569.e7 (2022).

61. B. Fauvet, *et al.*, Bacterial Hsp90 Facilitates the Degradation of Aggregation-Prone Hsp70-Hsp40 Substrates. *Front. Mol. Biosci.* **8**, 653073 (2021).

62. K. Bhattacharya, *et al.*, The Hsp70-Hsp90 co-chaperone Hop/Stip1 shifts the proteostatic balance from folding towards degradation. *Nat. Commun.* **11**, 5975 (2020).

63. M. E. Rebeaud, S. Mallik, P. Goloubinoff, D. S. Tawfik, On the evolution of chaperones and cochaperones and the expansion of proteomes across the Tree of Life. *Proc. Natl. Acad. Sci. U. S. A.* **118**, e2020885118 (2021).

64. C. Bordi, C. Iobbi-Nivol, V. Méjean, J.-C. Patte, Effects of ISSo2 insertions in structural and regulatory genes of the trimethylamine oxide reductase of Shewanella oneidensis. *J. Bacteriol.* **185**, 2042–2045 (2003).

65. P. Martin, *et al.*, Interplay between siderophores and colibactin genotoxin biosynthetic pathways in Escherichia coli. *PLoS Pathog.* **9**, e1003437 (2013).

66. N. J. Maillot, F. A. Honoré, Byrne, Deborah, V. Méjean, O. Genest, Cold adaptation in the environmental bacterium Shewanella oneidensis is controlled by a J-domain co-chaperone protein network. *Commun. Biol.* **2**, 323 (2019).

Legends

Fig. 1. Model of the collaboration between Hsp90 and DnaK. (A) Simplified schematic of the collaboration between bacterial Hsp90 and DnaK to remodel clients from *in vitro* reactivation assays. An unfolded protein recognized by a J-domain protein (not represented here) is addressed to and partially remodeled by the ATP-dependent DnaK chaperone (step 1). Through a direct interaction between Hsp90 and DnaK, the client is transferred to Hsp90 (step 2). The ATP-dependent activity of Hsp90 completes client remodeling (step 3). The client released from Hsp90 can reach its native active conformation (step 4). (B) Alignment of residues from the middle domain of Hsp90 from *E. coli* ($Hsp90_{Ec}$) and from *Shewanella oneidensis* ($Hsp90_{So}$) using the Pairwise Sequence Alignment software from EMBL-EBI. Residues that were mutated in this study are highlighted in yellow. Secondary structures (from PDB 2ioq) are indicated above the sequence of $Hsp90_{Ec}$ with hatched boxes for α-helices and arrows for β-sheets. (C) Substitution mutants used in this study. Residues that were mutated in this study in $Hsp90_{So}$ are homologous to the ones mutated in $Hsp90_{Ec}$ (39). (D) Model of the structure of Hsp90 from *Shewanella oneidensis* obtained by the software Swiss model based on the structure of $Hsp90_{Ec}$ (PDB 2ioq). In one protomer, the N-terminal domain is colored in light blue, the middle domain in wheat, and the C-terminal domain in pink. The other protomer is colored in gray. Residues that were mutated in our study are colored as indicated. The image was prepared using PyMOL.

Fig. 2. Identification of $Hsp90_{So}$ mutants defective for DnaK binding. (A) Bacterial two-hybrid assays showing interactions between $Hsp90_{So}$ wild-type (WT) or mutants and $DnaK_{So}$. $Hsp90_{So}$ WT or mutants were fused to the T25 domain of *B. pertussis* adenylate cyclase. $DnaK_{So}$ was fused to the T18 domain. *E. coli* Bth101Δ*htpG* cells

co-produced T18-DnaK$_{So}$ and T25-Hsp90$_{So}$ WT or mutants. The interaction was monitored by the quantification of β-galactosidase activity. In the negative controls (-), the pT18 or pT25 vectors were used. Data from six replicates are shown as mean ± SD. Results of one-way ANOVA tests indicate that the differences measured (versus the interaction DnaK$_{So}$ - Hsp90$_{So}$ WT) are significant (****: p-value ≤ 0.0001). (B) Co-purification assays showing the interactions between DnaK$_{So}$ and Hsp90$_{So}$ wild-type or mutants. Hsp90$_{So}$ WT or mutant with a CBP-tag and DnaK$_{So}$ with a 6His-tag were produced in the *E. coli* MG1655Δ*htpG* strain from plasmids pCBP-*hsp90$_{So}$* wild-type (WT) or mutants, and p*dnaK$_{So}$*-6His (+). Negative controls were performed using pBad33-CBP (cont) or pBad24 (-). CBP-Hsp90$_{So}$ was purified on CBP affinity resin. Purified proteins (co-purification panel) and samples before purification (input panel) were analyzed by Western blot with anti-Hsp90 or anti-His antibodies. The Western blots shown are representative of three independent experiments.

Fig. 3. The collaboration between Hsp90 and DnaK is essential for growth at high temperature in *S. oneidensis*. (A) Bacterial growth on solid media of the Δ*hsp90$_{So}$* strains producing the Hsp90$_{So}$ mutants from plasmids. *S. oneidensis* wild-type (WT) or Δ*hsp90$_{So}$* strains containing the pBad33 vector (p) or the pBad33 plasmids coding for Hsp90$_{So}$ wild-type or mutants grown in liquid at 28°C were 10-fold serial diluted and spotted on LB plates containing 0.01 % arabinose. The plates were incubated for 24 h at 35°C. (B) Liquid growth of the same strains as in *A*. Cells were grown in microplates in LB medium containing 0.015 % arabinose incubated at 38°C with shaking. (C) Bacterial growth on solid media of the strains producing the Hsp90$_{So}$ mutants from the chromosome. *S. oneidensis* wild-type (WT), ***Δhsp90$_{So}$*** or containing mutations in the *htpG* gene in the chromosome (*hsp90$_{So}$* (R364C) and *hsp90$_{So}$*(G279A-K280A-R364C))

grown in liquid at 28°C were 10-fold serial diluted and spotted on LB plates. The plates were incubated for 24 h at 35°C. (D) Liquid growth of the strains used in *C*. Cells were grown in microplates in LB medium incubated at 38°C with shaking. In *A* and *C*, the plates are representative of three independent experiments. In *B* and *D*, data from at least three replicates are shown as mean ± SD.

Fig. 4. The collaboration between Hsp90 and DnaK is required for TilS activation and protection in *S. oneidensis*. (A) Schematic representation of the *in vivo* assay used to measure TilS activity. TilS is an enzyme that allows the maturation of $tRNA^{Ile}$ required for the translation of the AUA codon into isoleucine (Ile). To measure the activity of TilS, a sequence containing four ATA codons (coding for isoleucine) was inserted between the start codon of the reporter gene *lacZ* and its coding sequence. Translation of the β-galactosidase is therefore dependent of the activity of TilS. (B) *S. oneidensis* wild-type (WT), Δ$hsp90_{So}$ (Δ), $hsp90_{So}$(R364C), and $hsp90_{So}$(G279A-K280A-R364C) containing the p(AUA)*lacZ* or p*lacZ* plasmids were grown at 34°C, and 0.2 % arabinose was added. β-galactosidase activity was measured 2 hours later. Data from at least five replicates are shown as mean ± SD. (C) *S. oneidensis* wild-type (WT), Δ$hsp90_{So}$, $hsp90_{So}$(R364C), and $hsp90_{So}$(G279A-K280A-R364C) containing the p$lacZ\text{-}tilS_{6His}$ plasmid allowing the production of TilS with a 6His tag were grown at 34°C and 0.02 % arabinose was added. After 2 hours, samples were analyzed by Western blot using anti-His antibody. As a control, chromosomal $Hsp90_{So}$ was detected using anti-$Hsp90_{Ec}$ antibody. Anti-AtcJ antibody was used as neutral loading control. This Western blot is representative of three independent experiments. (D) Quantification of the Western blots shown in *C* using ImageJ software. TilS amount (pastel orange bars) and $Hsp90_{So}$ amount (hatched, gray bars) in the wild-type (WT)

strain were set to 100 %. Data from three replicates are shown as mean ± SD. In *B* and *D*, results of one-way ANOVA tests indicate whether the differences measured are significant (****: p-value ≤ 0.0001; ***: p-value ≤ 0.001) or not significant (ns, p-value > 0.05).

Fig. 5. The cooperation between Hsp90 and DnaK is essential for colibactin production in *E. coli*. (A) Schematic representation of the *in vivo* assay used to measure colibactin production by *E. coli*. Colibactin is not purifiable and thus is quantified by measuring its genotoxic effect on cells exposed to the producing bacteria. Genotoxicity is demonstrated by immuno-staining phosphorylated histone H2AX in HeLa cells, a quantitative marker of DNA damage. (B) HeLa cells were exposed 4 h to the indicated *E. coli* strains with or without the pBad33 vector (p) or the pBad33 plasmids coding for $Hsp90_{Ec}$ wild-type or mutants, then DNA damage was quantified using anti-p-H2AX followed by fluorescent secondary antibodies and detection in a fluorescence plate reader. Data from three replicates are shown as mean ± SD. Results of one-way ANOVA tests indicate whether the differences measured are significant (****: p-value ≤ 0.0001; **: p-value ≤ 0.01; *: p-value ≤ 0.05) or not significant (ns, p-value > 0.05).

A

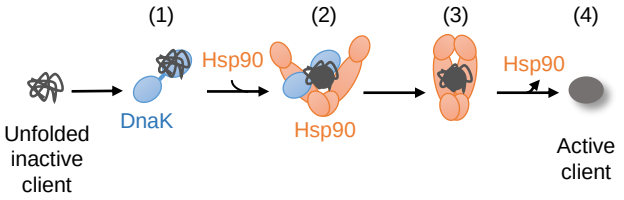

B

C

	Hsp90 residues		
$Hsp90_{Ec}$	K238C	G270A-K271A	R355C
$Hsp90_{So}$	K247C	G279A-K280A	R364C

D

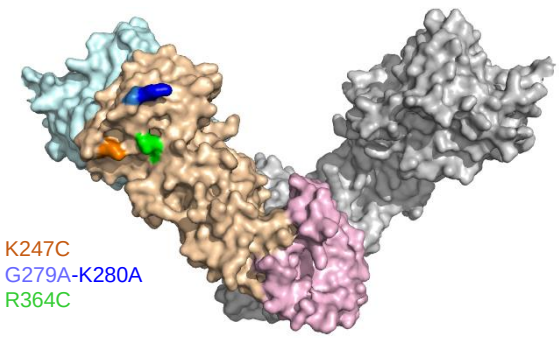

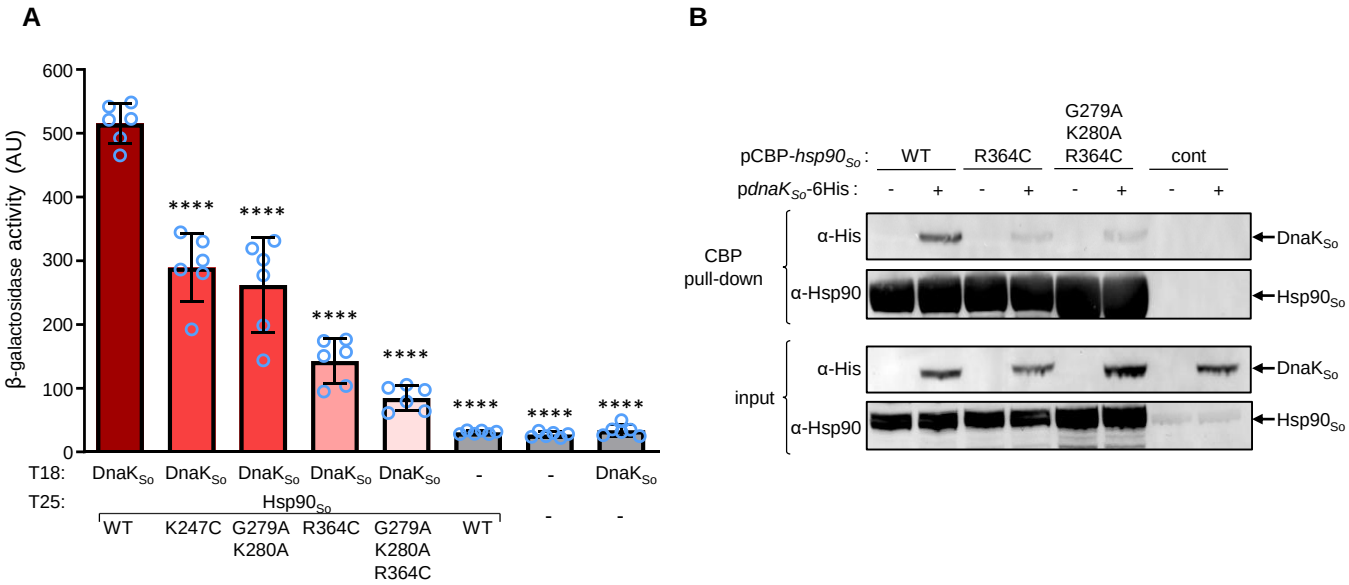
A
β-galactosidase activity (AU)
600
500
400
300
200
100
0
****
T18:
T25:
DnaK$_{So}$
Hsp90$_{So}$
WT
K247C
G279A K280A
R364C
G279A K280A R364C
B
pCBP-*hsp90*$_{So}$:
WT
R364C
G279A K280A R364C
cont
p*dnaK*$_{So}$-6His :
CBP pull-down
input
α-His
α-Hsp90
DnaK$_{So}$
Hsp90$_{So}$

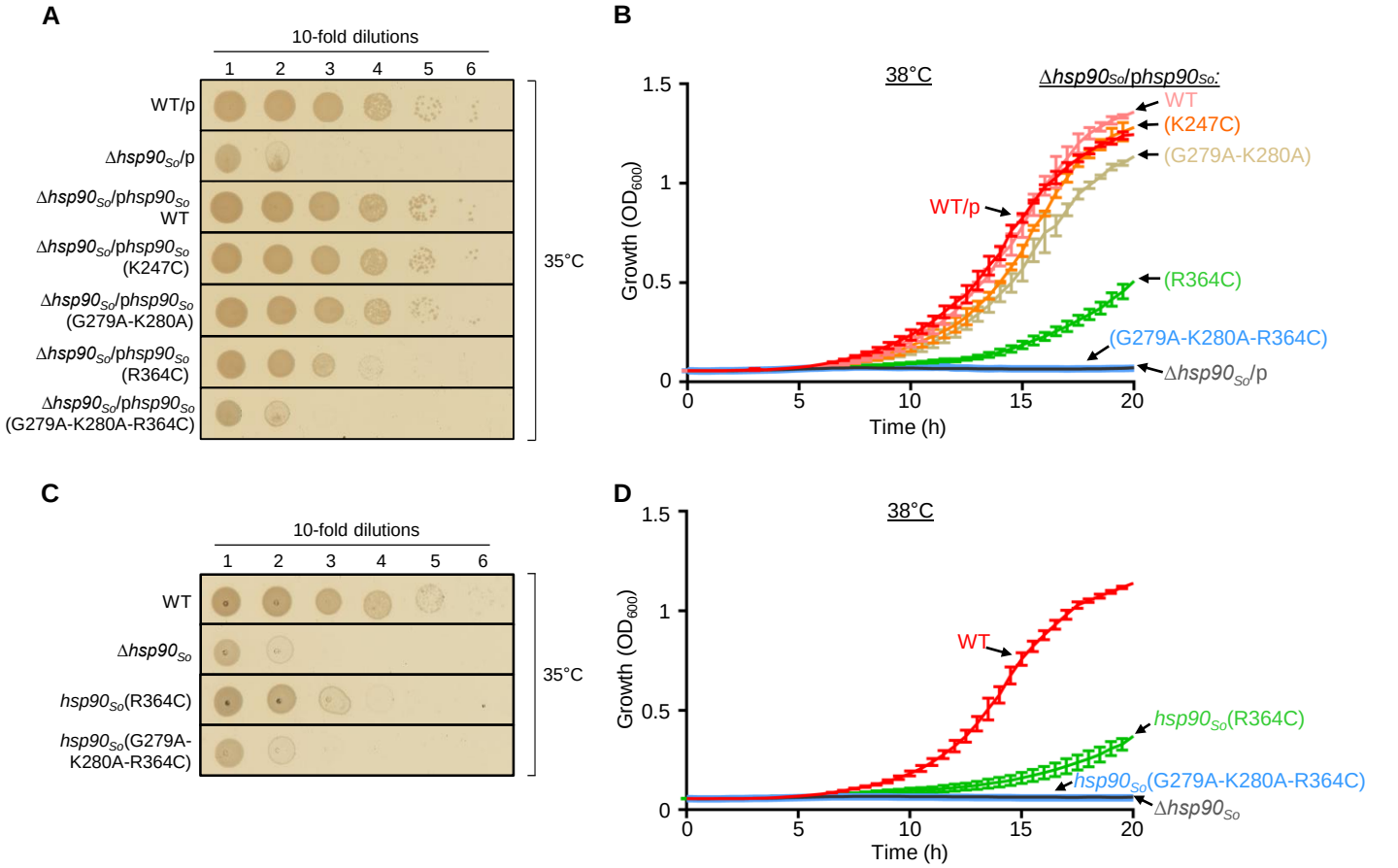
A
10-fold dilutions
1 2 3 4 5 6
WT/p
Δhsp90So/p
Δhsp90So/phsp90So WT
Δhsp90So/phsp90So (K247C)
Δhsp90So/phsp90So (G279A-K280A)
Δhsp90So/phsp90So (R364C)
Δhsp90So/phsp90So (G279A-K280A-R364C)
35°C
B
38°C
Δhsp90So/phsp90So:
WT
(K247C)
(G279A-K280A)
WT/p
(R364C)
(G279A-K280A-R364C)
Δhsp90So/p
Growth (OD600)
Time (h)
C
10-fold dilutions
1 2 3 4 5 6
WT
Δhsp90So
hsp90So(R364C)
hsp90So(G279A-K280A-R364C)
35°C
D
38°C
WT
hsp90So(R364C)
hsp90So(G279A-K280A-R364C)
Δhsp90So
Growth (OD600)
Time (h)

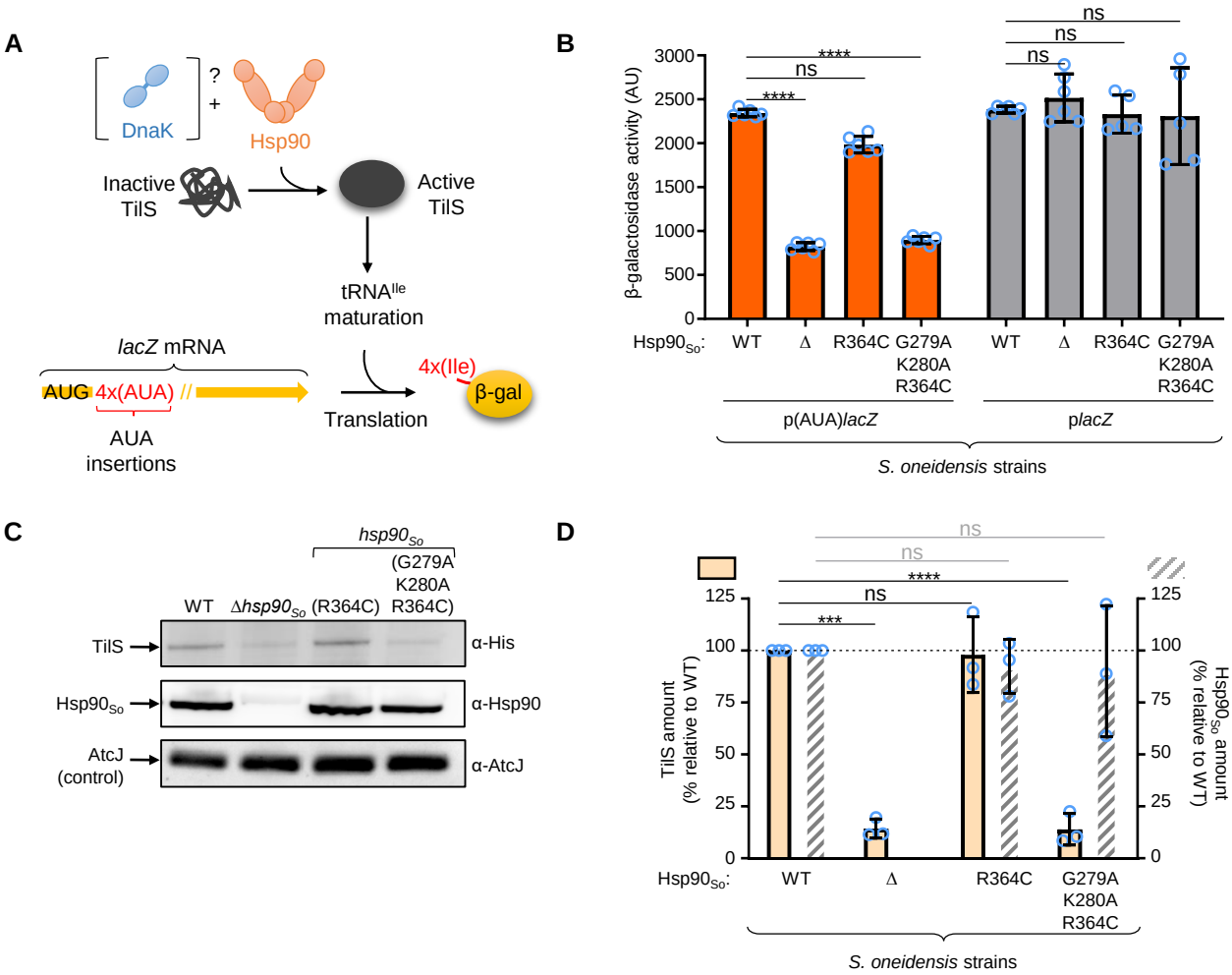
A
DnaK
?
+
Hsp90
Inactive TilS
Active TilS
tRNA^Ile maturation
lacZ mRNA
AUG 4x(AUA) //
AUA insertions
Translation
4x(Ile)
β-gal
B
β-galactosidase activity (AU)
3000
2500
2000
1500
1000
500
0
****
ns
****
ns
ns
ns
Hsp90So:
WT
Δ
R364C
G279A K280A R364C
WT
Δ
R364C
G279A K280A R364C
p(AUA)lacZ
placZ
S. oneidensis strains
C
hsp90So (G279A K280A R364C)
WT
ΔhspSo (R364C)
TilS
Hsp90So
AtcJ (control)
α-His
α-Hsp90
α-AtcJ
D
ns
ns
****
ns
***
TilS amount (% relative to WT)
Hsp90So amount (% relative to WT)
125
100
75
50
25
0
Hsp90So:
WT
Δ
R364C
G279A K280A R364C
S. oneidensis strains

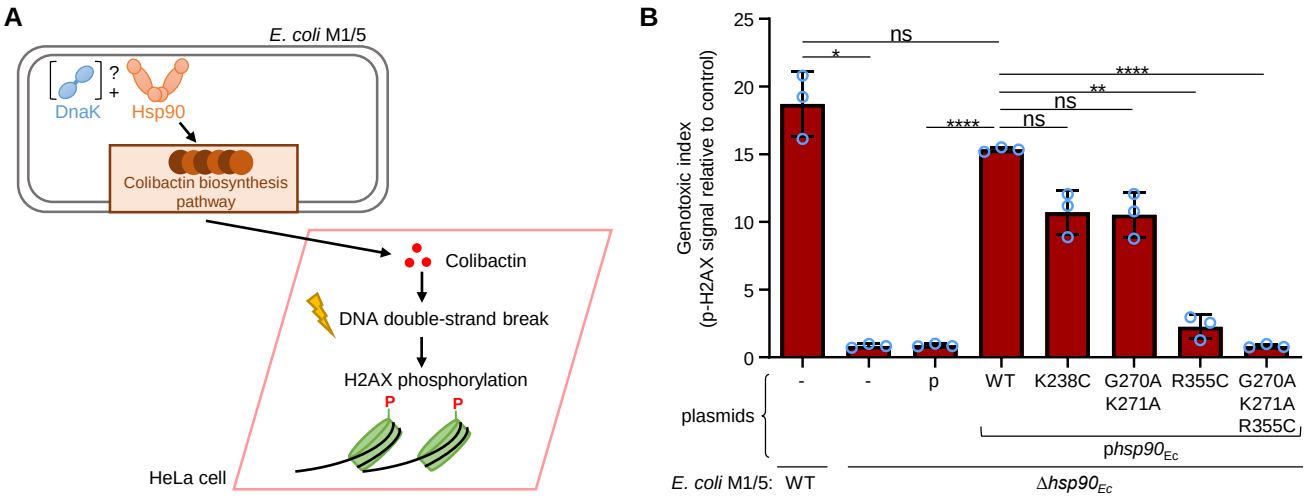
A
E. coli M1/5
?
+
DnaK
Hsp90
Colibactin biosynthesis pathway
Colibactin
DNA double-strand break
H2AX phosphorylation
P
P
HeLa cell
B
Genotoxic index (p-H2AX signal relative to control)
25
20
15
10
5
0
ns
*
****
**
ns
****
ns
-
-
p
WT
K238C
G270A K271A
R355C
G270A K271A R355C
plasmids
phsp90Ec
E. coli M1/5: WT
Δhsp90Ec

Supporting Results

Mutations in the region of DnaK involved in Hsp90 and DnaJ binding.

We tested whether mutations in the Hsp90 binding region of DnaK could affect growth under heat stress and TilS activation in *S. oneidensis*, as observed with the $Hsp90_{So}$ mutants described in this study. This region, which has been defined using *E. coli* Hsp90 and DnaK, comprises residues in the NBD of DnaK and overlaps with the DnaJ binding region (Fig. S7A) (1). Based on already characterized *E. coli* DnaK mutants (1), we constructed homologous mutants in DnaK from *S. oneidensis* (Fig. S7B). The interaction between $Hsp90_{So}$ wild-type and the $DnaK_{So}$ mutants was tested by two-hybrid and co-purification experiments. We found that $DnaK_{So}$(E216A-V217A) had reduced binding with $Hsp90_{So}$ in the two interaction assays, whereas the N169A-T172A mutation did not significantly reduced binding by two-hybrid (Fig. S7C-F).

To test the effects of DnaK mutations *in vivo*, homologous recombination was used to introduce the E216A-V217A mutations in the *dnaK* gene in the chromosome of *S. oneidensis*. We controlled that $DnaK_{So}$(E216A-V217A) was produced at the same level as $DnaK_{So}$ wild-type by Western blot (Fig. S8A). In growth conditions in which the collaboration $DnaK_{So}$-$Hsp90_{So}$ is not required, *i. e.* 28°C, the strain that produces $DnaK_{So}$(E216A-V217A) grew similarly to the wild-type strain on plates and in liquid cultures (Fig. S8B and D). These results indicate that, in conditions where $Hsp90_{So}$ is not required (28°C), the mutation E216A-V217A does not prevent $DnaK_{So}$ function, probably including the functional interaction with DnaJ. Indeed, DnaK and DnaJ are essential in *S. oneidensis* at permissive temperature as described in the literature (2, 3), and accordingly we did not succeed in deleting either the $dnaK_{So}$ gene alone, or the $dnaKJ_{So}$ operon. However, under heat stress, *i. e.* when the collaboration between DnaK and Hsp90 is required, growth of the strain producing $DnaK_{So}$(E216A-V217A) mutant was partially reduced on plates and delayed in liquid cultures (Fig. S8C and E). Interestingly, the activity of TilS was also reduced in the presence of $DnaK_{So}$(E216A-V217A) only at sub-lethal temperature, again strongly suggesting that the collaboration between DnaK and Hsp90 is essential for TilS activity (Fig. S8F and G).

Since the region of DnaK involved in Hsp90 binding overlaps with the one involved in DnaJ binding, we tested whether the mutations impair or not the *in vivo* function of DnaK independently of Hsp90. To do

that, we used an *E. coli* W3110 strain deleted of the *dnaK* and *dnaJ* genes (W3110Δ*dnaK-dnaJ*) (4). This strain shows a growth defect under heat stress, and we took advantage of the fact that Hsp90 - and therefore the collaboration Hsp90-DnaK - is known to be dispensable in *E. coli* even under heat stress (5). Plasmids allowing the production of DnaK wild-type or mutant and DnaJ from *E. coli* (p*dnaKdnaJ*$_{Ec}$) and from *S. oneidensis* (p*dnaKdnaJ*$_{So}$) were introduced in this strain. At permissive temperature, 28°C, all the strains grew similarly (Fig. S8H). At 42°C, growth of the W3110Δ*dnaK-dnaJ* strain with an empty vector was strongly reduced compared to the wild-type strain (Fig. S8I). Even if for unknown reasons, growth of the W3110Δ*dnaK-dnaJ* producing wild-type DnaK and DnaJ from *E. coli* or from *S. oneidensis* was only partially rescued, DnaK$_{So}$(E216A-V217A) produced from plasmid complemented the growth defects similarly to wild type DnaK$_{So}$ (Fig. S8I).

However, these results have to be taken with caution. Indeed, in the literature, the equivalent mutant from *E. coli*, DnaK$_{Ec}$(E217A-V218A), is altered *in vitro* for DnaJ binding, luciferase reactivation, and it leads to partial *in vivo* growth defects in *E. coli* under heat stress (6). Nonetheless, another study indicates that *in vitro* it reactivates another denatured model substrate, GFP, similarly to wild-type DnaK in the presence of DnaJ and GrpE (1). Therefore, although our results with the DnaK point mutant reinforce the hypothesis of the *in vivo* direct collaboration between Hsp90 and DnaK, we cannot exclude that the defects observed with this mutant in growth and in TilS activation could also result from defects in the collaboration between DnaK and DnaJ.

Supporting Materials and Methods

***S. oneidensis* strain constructions.** The *S. oneidensis hsp90*$_{So}$(R364C), *hsp90*$_{So}$(G279A-K280A-R364C), and *dnaK*$_{So}$(E216A-V217A) strains (Table S1) were constructed using homologous recombination as previously described with some modifications (7). Briefly, a fragment of the gene of interest centered on the mutation was PCR-amplified and cloned into the suicide pKNG101 vector, subsequently introduced by transformation into the CC118λpir strain. For the *hsp90*$_{So}$ mutants, the fragment was 1300 bp long. Since *dnaK* is essential in *S. oneidensis* (2), a copy of *dnaK*$_{So}$ (WT or mutant) and *dnaJ*$_{So}$ genes had to be present during all the homologous recombination process. To do that, the whole *dnaK*$_{So}$ gene with its promoter, along with the *dnaJ*$_{So}$ sequence were cloned in the pKNG101 vector. The resulting fragment was about 3700 bp long. The cloning step as well as the

insertion of the mutation were performed using the NEBuilder® HiFi DNA Assembly kit (NEB) according to the manufacturer protocol. The resulting plasmids were then introduced in *S. oneidensis* by conjugation. After integration into the chromosome, plasmids were removed using sucrose, resulting in only one copy of the mutated *dnaK*$_{So}$ gene. The substitutions were confirmed by PCR using forward primers with a 3' extremity hybridizing only on the mutated *hsp90*$_{So}$ or *dnaK*$_{So}$ sequence. The presence of the mutations was confirmed by sequencing.

Plasmid constructions. The pT18-*dnaK*$_{So}$ plasmid coding for DnaK$_{So}$ fused to the C-terminal extremity of the T18 domain of the adenylate cyclase of *B. pertussis* was used for two-hybrid experiments. It was constructed by amplifying by PCR the *dnaK* gene from the chromosome of *S. oneidensis* MR-1 using a forward oligonucleotide with the PstI restriction site, and a reverse oligonucleotide with the XbaI restriction site. After digestion, the DNA fragment was inserted into the pUT18C-linker vector (8) digested with the corresponding restriction enzymes. To construct the pT25-dnaK$_{So}$ plasmid, the same procedure as above was used except that the *dnaK*$_{So}$ gene was cloned into the pKT25-linker (8).

For co-purification experiments, the p*dnaK*$_{So}$-6His plasmid coding for the DnaK protein with a 6-histidine tag at the C-terminal extremity was constructed by amplifying by PCR the *dnaK* gene from the chromosome of *S. oneidensis* MR-1 using forward and reverse oligonucleotides with the KpnI and PstI restriction sites, respectively. A Shine-Dalgarno sequence was added on the forward oligonucleotide, and a sequence coding for a 6-histidine tag was added on the reverse oligonucleotide. After digestion, the DNA fragment was inserted into the pBad24 vector (9) digested with the corresponding restriction sites.

The pBad33-CBP plasmid was constructed by adding the sequence coding for the CBP tag from the pBAD24-CBP-linker (10) into the pBad33 vector (9). Plasmid pCBP-*hsp90*$_{So}$ was constructed by amplifying the *htpG* gene from the chromosome of *S. oneidensis* MR-1 using forward and reverse oligonucleotides with the XbaI and XhoI restriction sites, respectively. The digested DNA fragment was cloned into the pBad33-CBP plasmid, in frame with a sequence coding for a CBP tag at the N-terminal extremity of Hsp90$_{So}$.

The p*hsp90*$_{Ec}$ plasmid was constructed by digesting pET-HtpG (11) with XbaI/HindIII restriction enzymes and the resulting htpG-containing DNA fragment was cloned into similarly digested pBAD33.

The plasmids p*dnaKdnaJ*$_{Ec}$ and p*dnaKdnaJ*$_{So}$ were obtained by PCR amplification of the *dnaK*$_{Ec}$ and *dnaJ*$_{Ec}$ or *dnaK*$_{So}$ and *dnaJ*$_{So}$ genes from the chromosomes of *E. coli* MG1655 and *S. oneidensis* MR1-R, respectively. The resulting fragments were cloned into the pBad33 vector using NEBuilder Assembly kit (NEB). All plasmid constructions were verified by sequencing.

Proteins and *in vitro* assays. Production and purification of Hsp90$_{So}$ wild-type or mutant (12) and L2 (13) were performed as described previously. Concentrations are given as monomeric proteins.

ATP hydrolysis was measured at 37°C using a coupled ATP/NADH assay (13) using 3 µM Hsp90$_{So}$ WT or mutant and 2 µM L2. Far-UV circular dichroism spectroscopy of 3 µM Hsp90$_{So}$ WT, R364C and G279A-K280A-R364C was performed in 20 mM phosphate buffer, pH 7.4, using a Jasco-815 spectropolarimeter at 25°C and 37°C. For size exclusion chromatography, 30 µM of purified Hsp90$_{So}$ WT, R364C and G279A-K280A-R364C in 50mM Tris-HCl pH 7.5, 100 mM KCl, 10 % glycerol, 1 mM DTT (buffer B) were analyzed on a Superdex 200 Increase 10/300 GL column (GE healthcare). Light scattering experiments were performed as previously described (12).

ITC experiments were performed at 25 °C using the MicroCal PEAQ-ITC (Malvern). The Hsp90$_{So}$ WT or mutants and DnaK$_{So}$ proteins were dialyzed overnight at 4°C in buffer B to avoid discrepancies from buffer mismatch. In total, 500 µM of ligands (Hsp90$_{So}$ WT or mutants) with 1 mM ATP, were titrated using 19 injections of 2 µl against 10 µM of DnaK$_{So}$, 1 mM ATP in the ITC cell with a constant stirring speed of 750 rpm. Duplicates were performed for each measurement. Controls showing no interaction were performed by replacing each protein with buffer in the presence of ATP. The data were fitted using a “One Set of Sites” model in the PEAQ-ITC Analysis Software.

Complementation of *E. coli* Δ*dnaKdnaJ* strain. *E. coli* W3110 wild-type or Δ*dnaKdnaJ*$_{Ec}$ strains were transformed with pBad33 derived plasmids. The resulting strains were grown overnight at 28°C in LB with chloramphenicol. The strains were inoculated to OD_{600}=0.04 in LB with chloramphenicol and incubated at 28°C until late exponential phase. Cells were diluted to OD_{600}=1, and 3 µL of 10-time serial dilutions were spotted on LB-agar plates supplemented with 0.01 % arabinose. Plates were incubated at 28°C or 42°C.

A

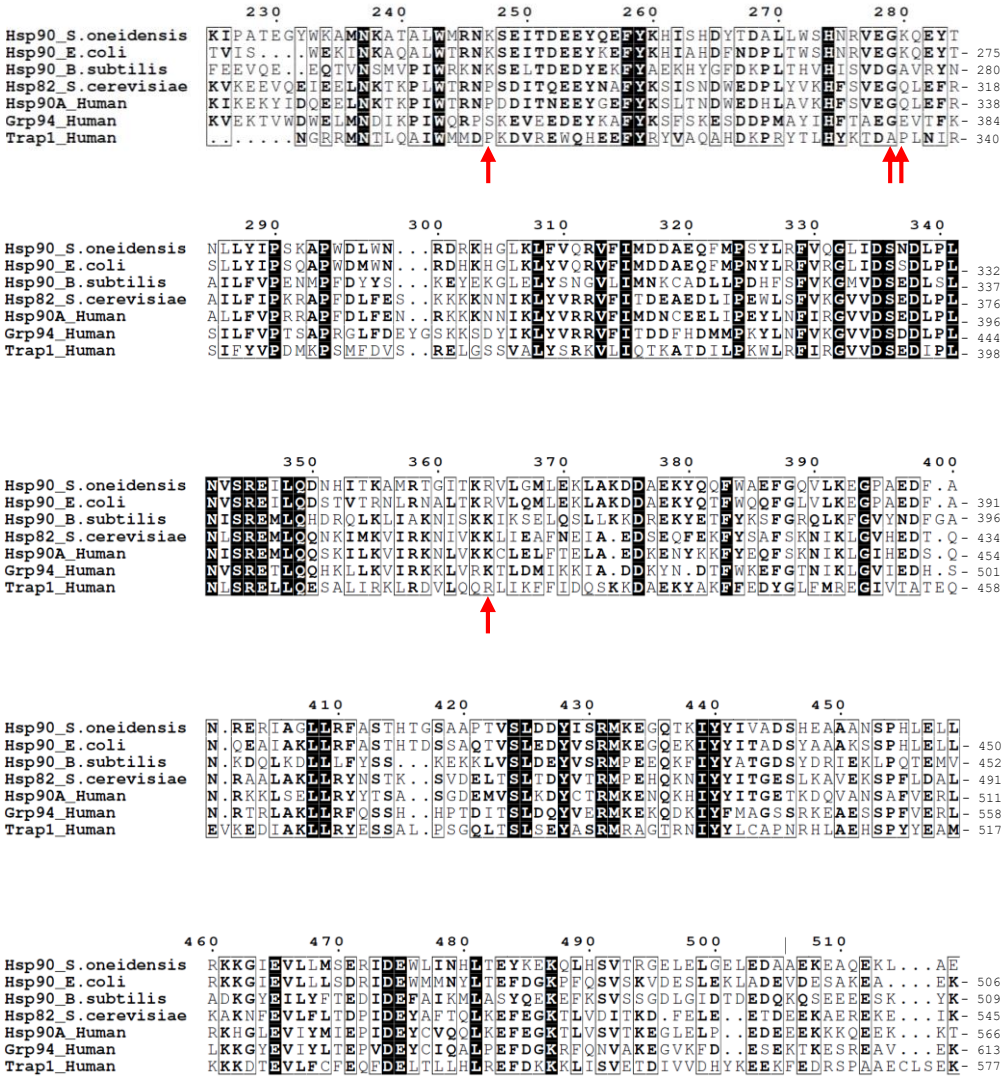

B

	Hsp90 residues		
Hsp90 *S. oneidensis*	K247	G279-K280	R364
Hsp90 *E. coli*	K238	G270-K271	R355
Hsp90 *B. subtilis*	K243	G275-A276	K360
Hsp82 *S. cerevisiae*	P281	G313-Q314	K399
Hsp90α (Human)	P301	G333-Q334	K419
Grp94 (Human)	S347	G379-E380	K467
Trap1 (Human)	P303	A335-P336	R421

Fig. S1. Conservation of the Hsp90 middle domain. (A) Sequence alignment of the middle domains (MD) of bacterial Hsp90 (*S. oneidensis*, *E. coli*, *B. subtilis*), yeast Hsp90 (Hsp82 from *S. cerevisiae*), and human Hsp90 (cytosolic Hsp90α, endoplasmic reticulum Grp94, and mitochondrial Trap1) using the multiple sequence alignment tool «Multalin» (http://multalin.toulouse.inra.fr/multalin/). The ESPript program (https://espript.ibcp.fr/ESPript/ESPript/) was used to display the alignment. Residues mutated in this study are pointed by red arrows. (B) The residues from several Hsp90 proteins homologous to the ones mutated in $Hsp90_{So}$ are indicated.

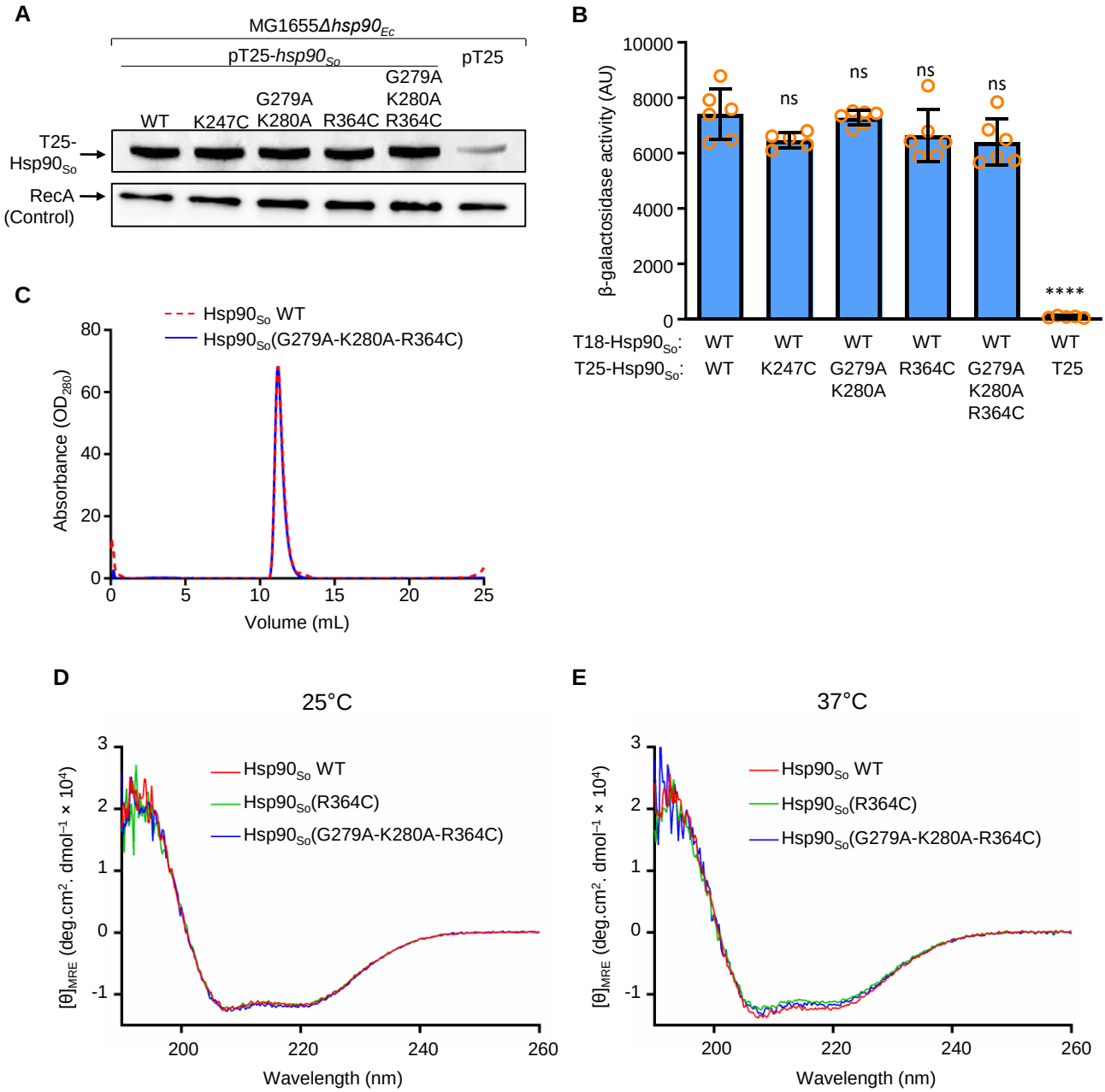

Fig. S2. The mutations did not alter Hsp90$_{So}$ properties other than DnaK binding. (A) Production of the T25-Hsp90$_{So}$ wild-type or mutant fusion proteins. The *E. coli* MG1655Δ*hsp90*$_{Ec}$ strains containing the pT25 vector or the plasmids pT25-*hsp90*$_{So}$ wild-type (WT) or mutants were grown overnight at 28°C with kanamycin and 1 mM IPTG. The samples were normalized and analyzed by Western blot. The T25-Hsp90$_{So}$ fusion proteins were detected using anti-Hsp90 antibody. Anti-RecA antibody was used as neutral loading control. (B) Bacterial two-hybrid assays showing dimer interactions between one protomer from Hsp90$_{So}$ wild-type (WT) and the other protomer from Hsp90$_{So}$ wild-type or mutant as indicated. Plasmids pT25-*hsp90*$_{So}$ wild-type (WT) or mutants were co-transformed with the pT18-*hsp90*$_{So}$ wild-type plasmid in the *E. coli* Bth101Δ*htpG*. The interaction was monitored by the quantification of the β-galactosidase activity in liquid assays as indicated in Material and Methods. Data from at least five replicates are shown as mean ± SD. Results of one-way ANOVA tests indicate whether the differences measured (vs WT-WT) are significant (****: p-value ≤ 0.0001) or not significant (ns, p-value > 0.05). (C) 30 µM of purified Hsp90$_{So}$ wild-type (WT) or Hsp90$_{So}$(G279A-K280A-R364C) were analyzed on a Superdex 200 Increase 10/300 GL size exclusion chromatography column. A representative result of several experiments is shown. (D-E) Far-UV circular dichroism spectra of 3 µM Hsp90$_{So}$ wild-type (WT), Hsp90$_{So}$(R364C), and Hsp90$_{So}$(G279A-K280A-R364C) were recorded at 25°C (D) and 37°C (E). MRE: mean residue ellipticity. A representative result of several experiments is shown.

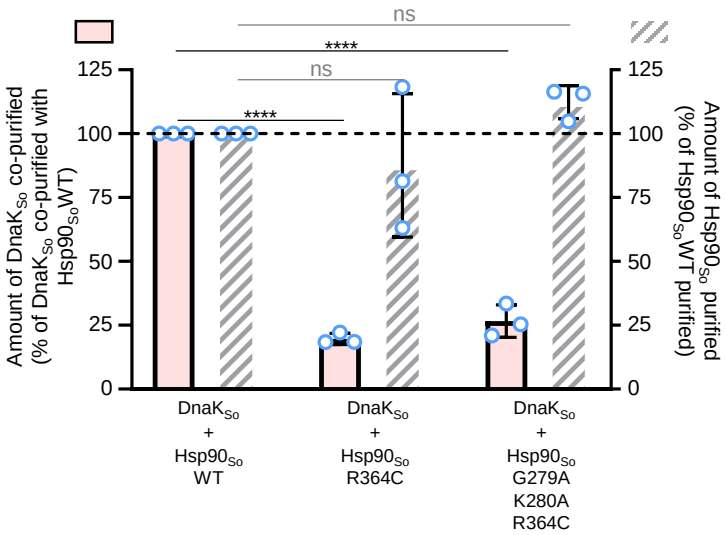

Fig. S3. Quantification of the co-purification experiment shown in Figure 2B. Quantification of the intensity of the bands observed in Fig. 2B was performed using the ImageJ software. The amount of DnaK$_{So}$ co-purified with Hsp90$_{So}$ is represented as pink bars, and 100 % corresponds to the amount of DnaK$_{So}$ co-purified with Hsp90$_{So}$ WT. The amount of Hsp90$_{So}$ retained on the calmodulin beads is shown as hatched grey bars and the amount of Hsp90$_{So}$ WT retained was set to 100 %. Data from three replicates are shown as mean ± SD. Results of one-way ANOVA tests indicate whether the differences measured are significant (****: p-value ≤ 0.0001) or not significant (ns, p-value > 0.05).

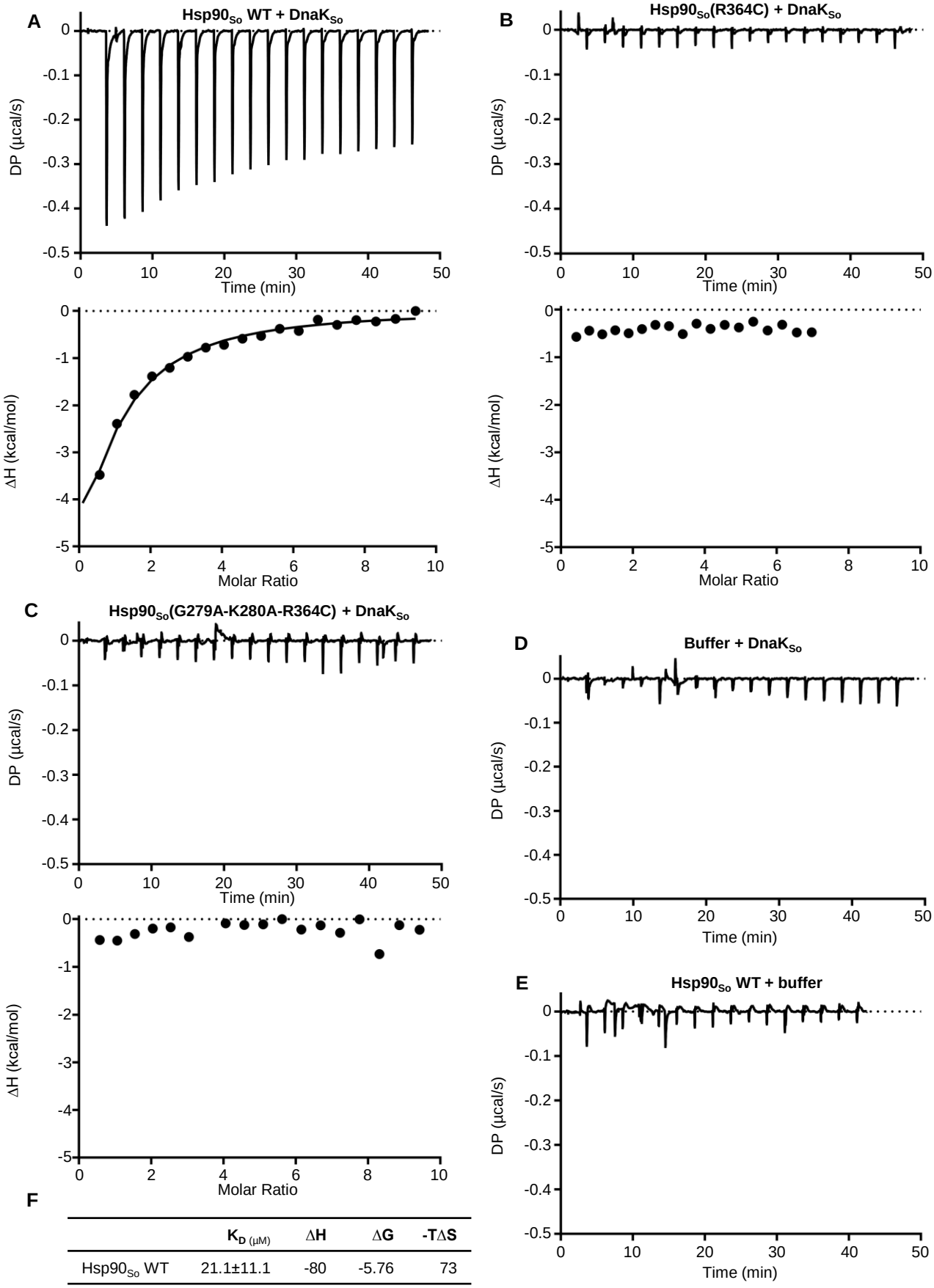

F

	$K_{D\ (\mu M)}$	ΔH	ΔG	-TΔS
$Hsp90_{So}$ WT	21.1±11.1	-80	-5.76	73

Fig. S4 : The $Hsp90_{So}$ mutants did not interact with $DnaK_{So}$ *in vitro* by isothermal titration calorimetry (ITC). (A-E) ITC experiments were performed on purified proteins. 500 µM $Hsp90_{So}$ wild-type (WT) (A), 370 µM $Hsp90_{So}$ R364C (B), and 500 µM $Hsp90_{So}$ G279A-K280A-R364C (C) with 10 µM $DnaK_{So}$ in 50 mM Tris-HCl pH 7.5, 100 mM KCl, 10 % glycerol, 1 mM DTT and 1 mM ATP were used. (D) Control experiment with 10 µM $DnaK_{So}$ + buffer. (E) Control experiment with 500 µM $Hsp90_{So}$ WT + buffer. In *A-E*, data shown are representative of at least two independent experiments. (F) Table with binding constant and thermodynamic parameters of $DnaK_{So}$ and $Hsp90_{So}$ WT in the presence of ATP, K_D shows the deviation within the measurement with 19 injections.

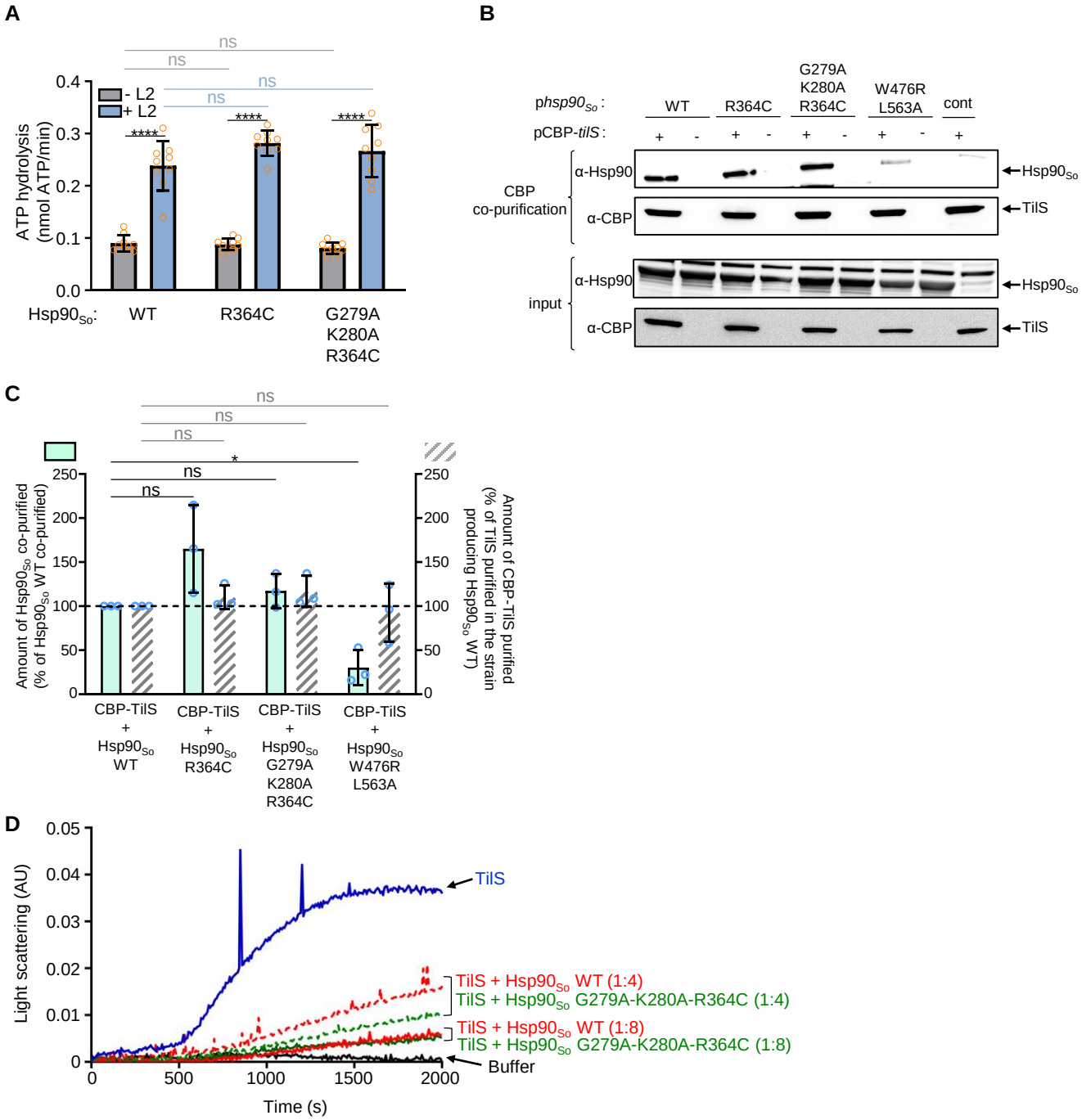

Fig. S5. Hsp90$_{So}$ mutants are not impaired in client binding. (A) Measurement of the basal and client-stimulated ATPase activity of Hsp90$_{So}$ wild-type (WT), Hsp90$_{So}$(R364C), and Hsp90$_{So}$(G279A-K280A-R364C). ATP hydrolysis by 3 µM Hsp90$_{So}$ wild-type or mutants in the presence or absence of 2 µM L2 was measured *in vitro* at 37°C as described in Material and Methods. Data from nine replicates are shown as mean ± SD. Results of one-way ANOVA tests indicate whether the differences measured are significant (****: p-value ≤ 0.0001) or not significant (ns, p-value > 0.05). (B) Co-purification assays showing the interactions between TilS from *S. oneidensis* and Hsp90$_{So}$ wild-type or mutants. TilS with a CBP-tag and Hsp90$_{So}$ wild-type or mutants were produced in the *E. coli* MG1655Δ*htpG* strain from plasmids pCBP-*tilS* and p*hsp90*$_{So}$ wild-type (WT) or mutants. Negative controls were performed using the Hsp90$_{So}$ mutant W476R-L563A affected for client binding, pBad24-CBP (-) or pBad33 (cont). CBP-TilS was purified on CBP affinity resin. Purified proteins (CBP co-purification panel) and samples before purification (input panel) were analyzed by Western blot with anti-CBP or anti-Hsp90 antibodies. The Western blots shown are representative of three independent experiments. (C) Quantification of the Western blots shown in *B* was performed using the ImageJ software. The amount of Hsp90$_{So}$ co-purified with CBP-TilS is represented as pastel green bars, and 100% corresponds to the amount of Hsp90$_{So}$ WT co-purified with CBP-TilS. The amount of CBP-TilS retained on the calmodulin beads is shown as hatched gray bars and the amount of CBP-TilS retained in the strain producing Hsp90$_{So}$ WT was set to 100%. Data from three replicates are shown as mean ± SD. Results of one-way ANOVA tests indicate whether the differences measured are significant (*: p-value ≤ 0.05) or not significant (ns, p-value > 0.05). (D) Light scattering experiments showing that Hsp90$_{So}$ WT and Hsp90$_{So}$(G279A-K280A-R364C) similarly prevent aggregation of TilS. Purified TilS (2 µM) with or without purified Hsp90$_{So}$ WT or mutant (8 µM or 16 µM, dimeric Hsp90, as indicated) were incubated at 42°C and OD_{360} was measured with time. An increase in absorbance indicates that TilS aggregates. The graph shown is representative of three independent experiments.

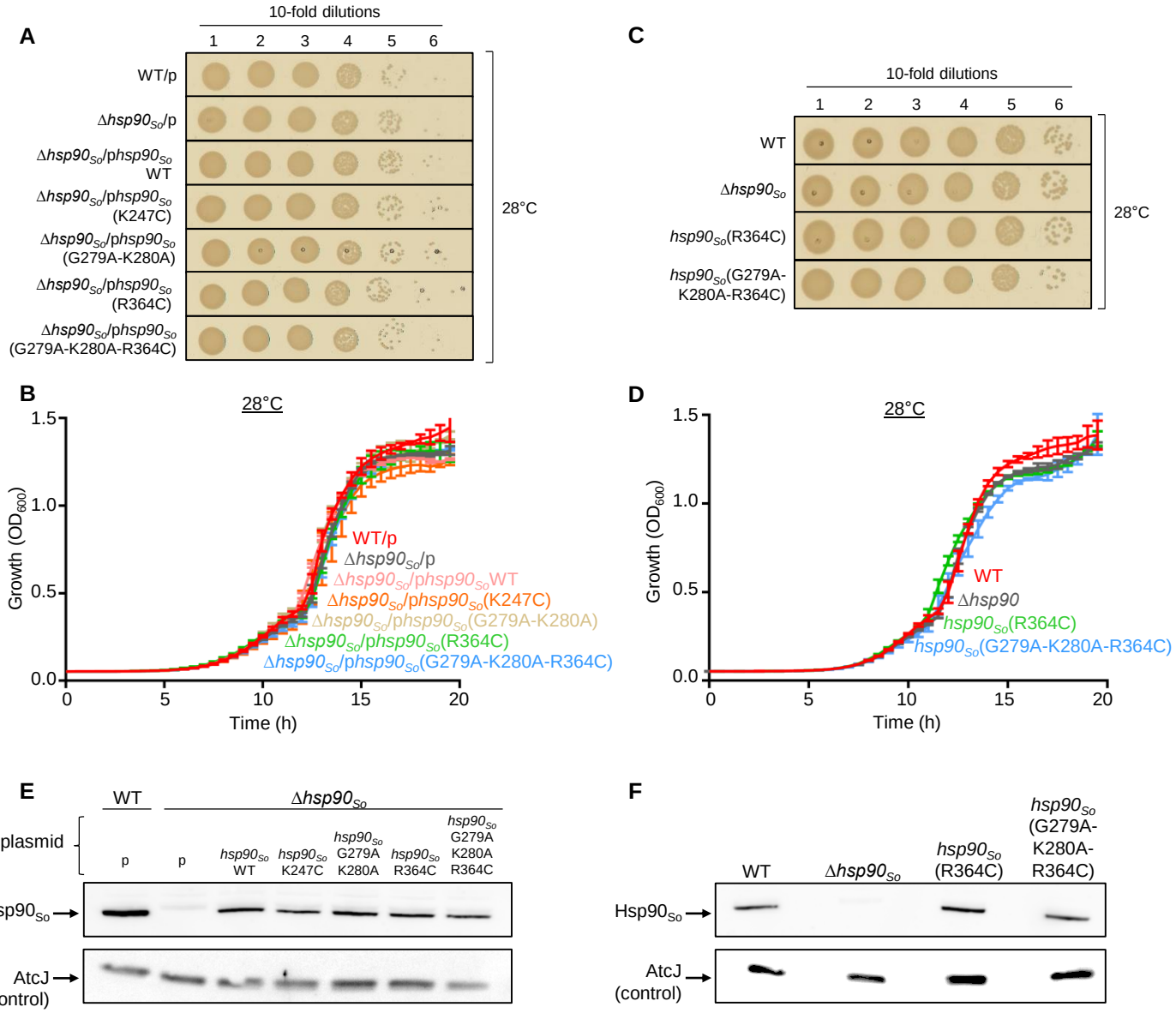

Fig. S6. Controls related to bacterial growth with the Hsp90$_{So}$ mutants. (A) Bacterial growth on solid media of the Δ*hsp90*$_{So}$ strains producing the Hsp90$_{So}$ single mutants from plasmids. *S. oneidensis* wild-type (WT) or Δ*hsp90*$_{So}$ strains containing the pBad33 vector (p) or the pBad33 plasmids coding for Hsp90$_{So}$ wild type or mutants grown in liquid at 28°C were 10-fold serial diluted and spotted on LB plates containing 0.01 % arabinose. The plates were incubated overnight at 28°C. (B) Liquid growth of the same strains as in *A*. Cells were grown in microplates in LB medium containing 0.015% arabinose incubated at 28°C with shaking. (C) Bacterial growth on solid media of the strains producing the Hsp90$_{So}$ single mutants from the chromosome. *S. oneidensis* wild-type (WT), *Δhsp90*$_{So}$ or containing mutations in the *htpG* gene in the chromosome (*hsp90*$_{So}$ (R364C) and *hsp90*$_{So}$(G279A-K280A-R364C)) grown in liquid at 28°C were 10-fold serial diluted and spotted on LB plates. The plates were incubated overnight at 28°C. (D) Liquid growth of the *hsp90*$_{So}$ mutant strains as in *C*. Cells were grown in microplates in LB medium incubated at 28°C with shaking. In *A* and *C*, the plates are representative of three independent experiments. In *B* and *D*, data from at least three replicates are shown as mean ± SD. (E) Control of the production of the Hsp90$_{So}$ mutants produced from the plasmids. Strains as in *A* were grown at 28°C with chloramphenicol during 3 h, and 0.01 % arabinose was added. 2 hours later, the samples were normalized and analyzed on Western blot with anti-Hsp90 antibody. (F) Control of the production of the Hsp90$_{So}$ mutants produced from the chromosome. Strains as in *C* were grown at 28°C during 3 h, then the samples were normalized and analyzed on Western blot with anti-Hsp90 antibody. In *E* and *F*, Western blots are representative of three independent experiments. Anti-AtcJ antibody was used as neutral loading control and shows that same amount of protein was loaded in the different wells.

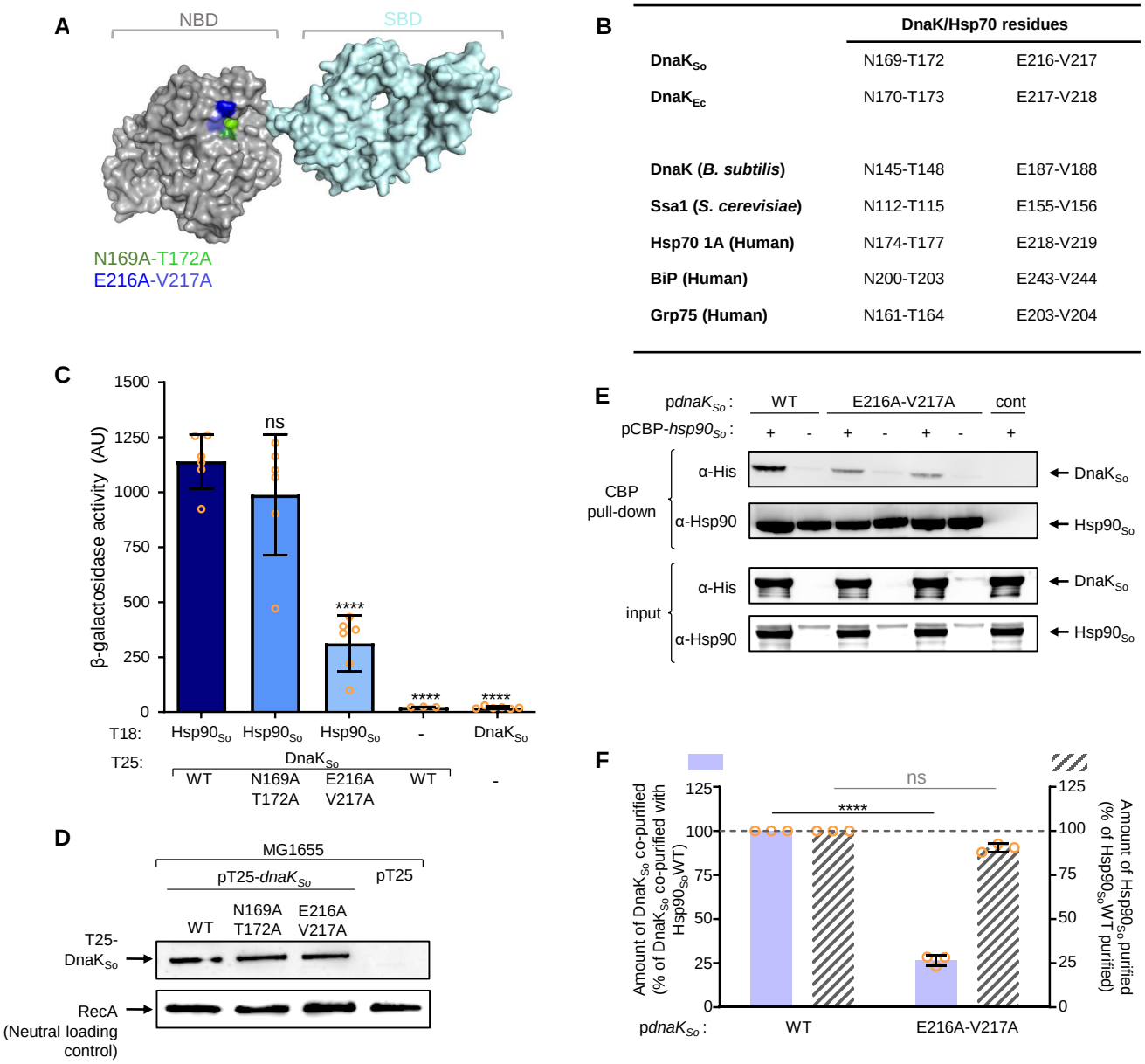

Fig. S7: Identification of DnaK mutants defective for Hsp90 binding. (A) Model of the structure of DnaK from *Shewanella oneidensis* obtained by the software Swiss model based on the structure of DnaK$_{Ec}$ (PDB 2KHO). The nucleotide-binding domain (NBD) is colored in gray and the substrate-binding domain (SBD) in light blue. Residues that were mutated in our study are colored as indicated. The image was prepared using PyMOL. (B) The residues from several Hsp70/DnaK proteins homologous to the ones mutated in DnaK$_{So}$ in this study are indicated. (C) Bacterial two-hybrid assays showing interactions between DnaK$_{So}$ wild-type (WT) or mutants and Hsp90 from *S. oneidensis*. DnaK$_{So}$ WT or mutants were fused to the T25 domain of *B. pertussis* adenylate cyclase. Hsp90 from *S. oneidensis* was fused to the T18 domain. *E. coli* Bth101Δ*htpG* cells co-produced T18-Hsp90$_{So}$ and T25-DnaK$_{So}$ WT or mutants. The interaction was monitored by the quantification of β-galactosidase activity. In the negative controls (-), the pT18 or pT25 vectors were used. Data from at least three replicates are shown as mean ± SD. Results of one-way ANOVA tests indicate whether the differences measured (vs Hsp90$_{So}$ - DnaK$_{So}$ WT) are significant (****: p-value ≤ 0.0001) or not significant (ns, p-value > 0.05). (D) Production of the T25-DnaK$_{So}$ wild-type or mutant fusion proteins. The *E. coli* MG1655*Δhsp90$_{Ec}$* strains containing the pT25 vector or the plasmids pT25-*dnaK$_{So}$* wild-type (WT) or mutants were grown overnight at 28°C with kanamycin and 1 mM IPTG. The samples were normalized and analyzed by Western blot. The T25-DnaK$_{So}$ fusion proteins were detected using anti-DnaK$_{So}$ antibody. Anti-RecA antibody was used as neutral loading control. (E) Co-purification assays showing the interactions between Hsp90 from *S. oneidensis* and DnaK$_{So}$ wild-type or mutants. Hsp90$_{So}$ with a CBP-tag and DnaK$_{So}$ WT or mutant with a 6His-tag were produced in the *E. coli* MG1655Δ*htpG* strain from plasmids pCBP-*hsp90$_{So}$*, and p*dnaK$_{So}$*-6His wild-type (WT) or mutants. Negative controls were performed using pBad33-CBP (-) or pBad24 (cont). CBP-Hsp90 was purified on CBP affinity resin. Purified proteins (CBP pull-down panel) and samples before purification (input panel) were analyzed by Western blot with anti-His or anti-Hsp90 antibodies. The Western blots shown are representative of three independent experiments. (F) Quantification of the Western blots shown in *E* was performed using the ImageJ software. The amount of DnaK$_{So}$ co-purified with Hsp90$_{So}$ is represented as purple bars, and 100 % corresponds to the amount of DnaK$_{So}$ WT co-purified with Hsp90$_{So}$. The amount of Hsp90$_{So}$ retained on the calmodulin beads is shown as hatched gray bars and the amount of Hsp90$_{So}$ retained in the strain producing DnaK$_{So}$ WT was set to 100 %. Data from three replicates are shown as mean ± SD. Results of one-way ANOVA tests indicate whether the differences measured are significant (****: p-value ≤ 0.0001) or not significant (ns, p-value > 0.05).

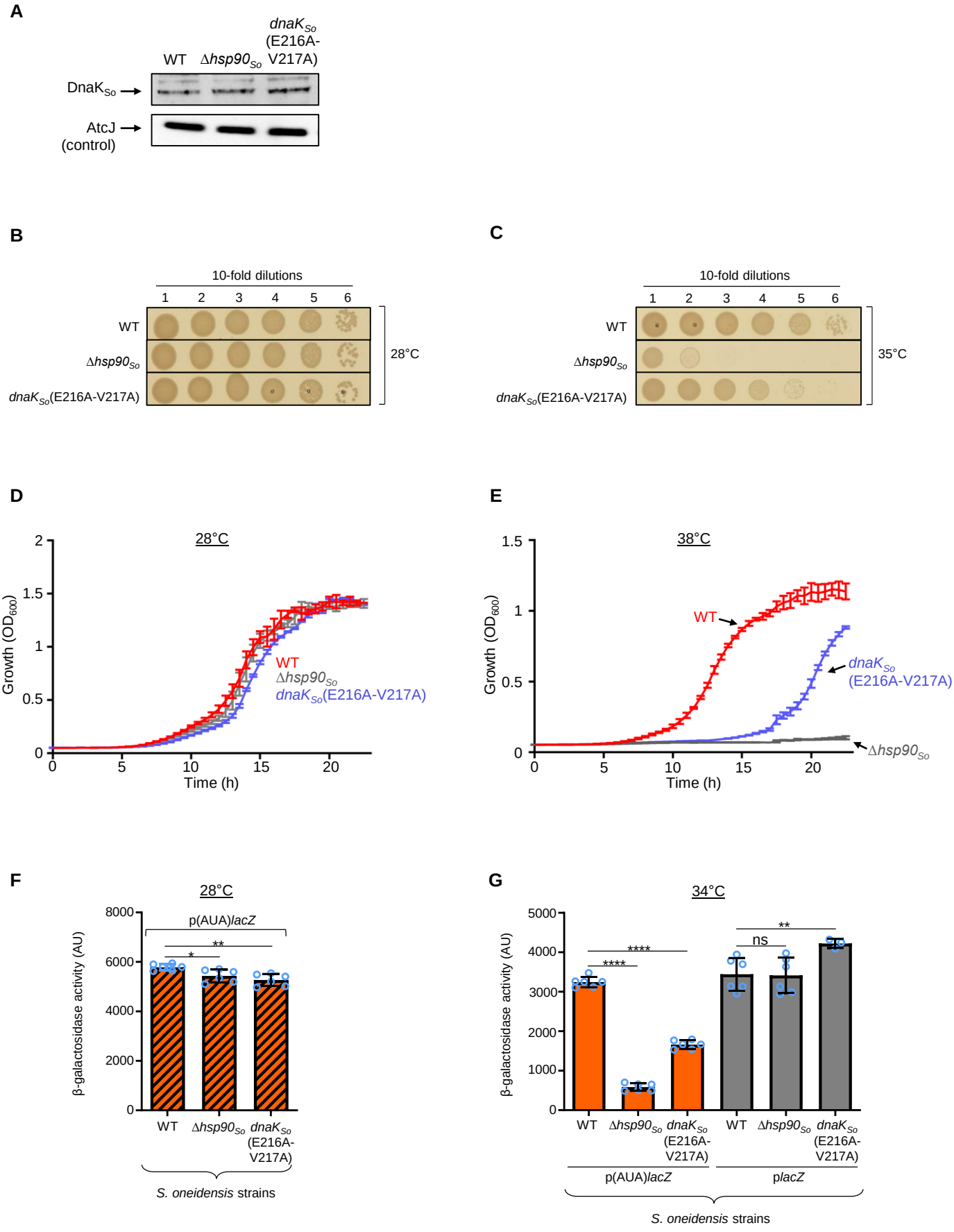

Fig. S8 (Legend next page)

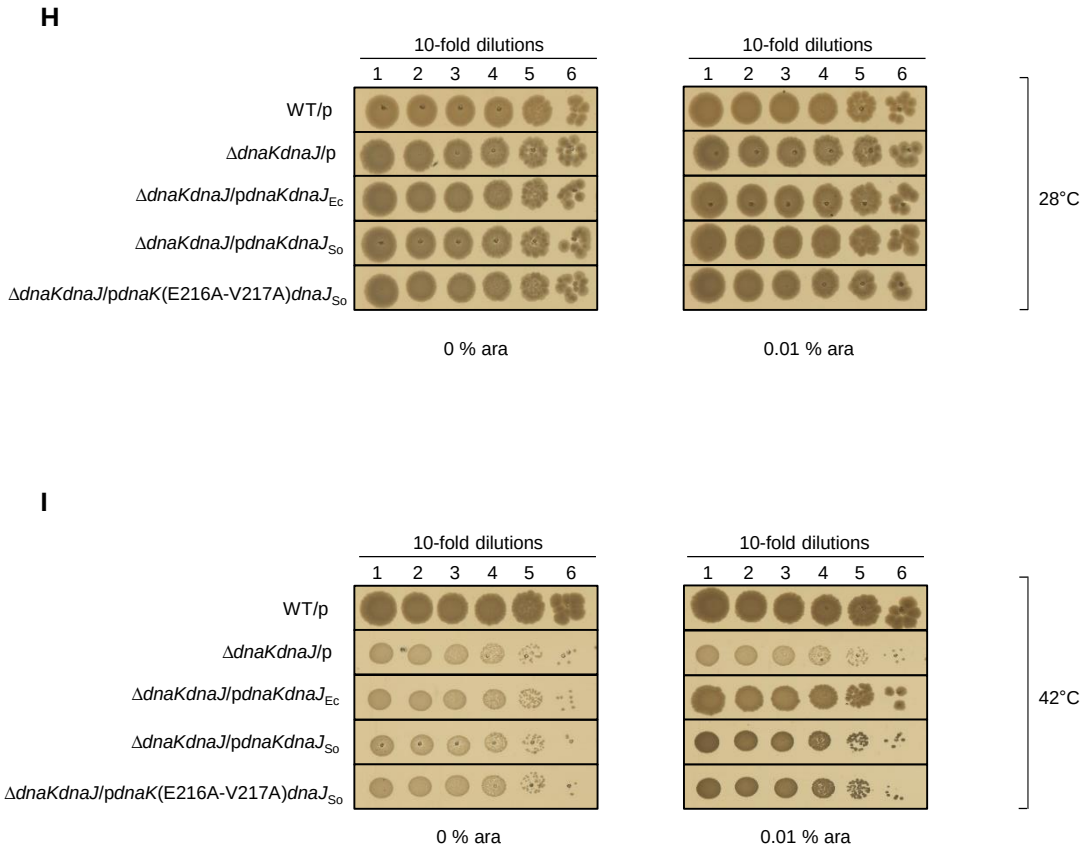

Fig. S8 (continued). The DnaK$_{So}$(E216A-V217A) mutant is affected for growth under heat stress and for TilS activation in *S. oneidensis*. (A) Control of the production of DnaK$_{So}$(E216A-V217A). *S. oneidensis* wild-type (WT), Δ*hsp90*$_{So}$, and *dnaK*$_{So}$(E216A-V217A) strains were grown at 28°C during 3 h, then the samples were normalized and analyzed on Western blot with anti-DnaK$_{So}$ antibody. Western blot is representative of three independent experiments. Anti-AtcJ antibody was used as neutral loading control and shows that same amount of protein was loaded in the different wells. (B-C) Bacterial growth on solid media of *S. oneidensis* wild-type (WT), *Δhsp90*$_{So}$, and *dnaK*$_{So}$(E216A-V217A). Strains grown in liquid at 28°C were 10-fold serial diluted and spotted on LB plates. The plates were incubated overnight at 28°C (B) or 37°C (C). (D-E) Bacterial growth in liquid media. Cells as in B were grown with shaking in microplates in LB medium incubated at 28°C (D) or 38°C (E). (F-G) *S. oneidensis* wild-type (WT), Δ*hsp90*$_{So}$ and *dnaK*$_{So}$(E216A-V217A) containing the p(AUA)*lacZ* or p*lacZ* plasmids were grown at 28°C (F) or 34°C (G), and 0.2 % arabinose was added. β-galactosidase activity was measured 2 hours later. (H-I) The DnaK$_{So}$(E216A-V217A) mutant supports *E. coli* growth under heat stress. The *E. coli* W3110 wild-type strain as well as the *E. coli* W3110Δ*dnaKdnaJ* strain containing the pBad33 vector (p) or the pBad33 plasmids coding for DnaK wild-type or mutant and DnaJ from *E. coli* or *S. oneidensis* were grown in liquid at 28°C. The cells were 10-fold serial diluted and spotted on LB plates without or with 0.01 % arabinose. Plates were incubated for 24 hours at 28°C (H) or 42°C (I). In *B*, *C*, *H* and *I* the plates are representative of three independent experiments. In *D-G*, data from at least three replicates are shown as mean ± SD. When indicated, results of one-way ANOVA tests indicate whether the differences measured are significant (****: p-value ≤ 0.0001; **: p-value ≤ 0.01; *: p-value ≤ 0.05) or not significant (ns, p-value > 0.05).

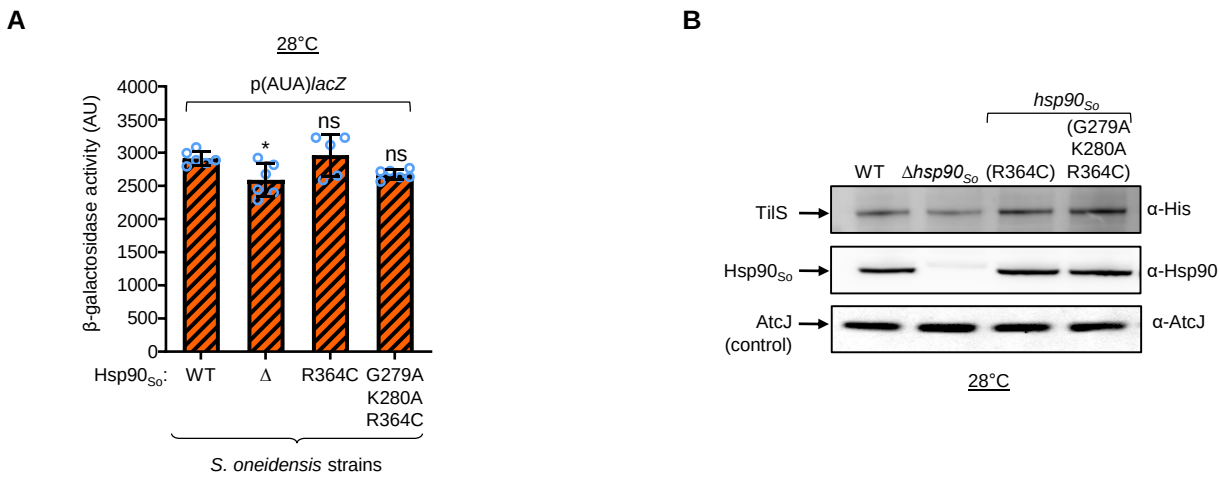

Fig. S9. Controls related to TilS activity and protection. (A) *S. oneidensis* wild-type (WT), Δ*hsp90*$_{So}$ (Δ), *hsp90*$_{So}$(R364C), and *hsp90*$_{So}$(G279A-K280A-R364C) containing the p(AUA)*lacZ* plasmid were grown at 28°C, and 0.2 % arabinose was added. β-galactosidase activity was measured 2 hours later. Data from at least five replicates are shown as mean ± SD. Results of one-way ANOVA tests indicate whether the differences measured (vs WT) are significant (*: p-value ≤ 0.05) or not significant (ns, p-value > 0.05). (B) *S. oneidensis* wild-type (WT), Δ*hsp90*$_{So}$, *hsp90*$_{So}$(R364C), and *hsp90*$_{So}$(G279A-K280A-R364C) containing the p*lacZ-tilS*$_{6His}$ plasmid allowing the production of TilS with a 6His tag were grown at 28°C and 0.02 % arabinose was added. After 2 hours, samples were analyzed by Western blot using anti-His antibody. As a control, chromosomal Hsp90$_{So}$ was detected using anti-Hsp90 antibody, and anti-AtcJ antibody was used as neutral loading control. This Western blot is representative of three independent experiments.

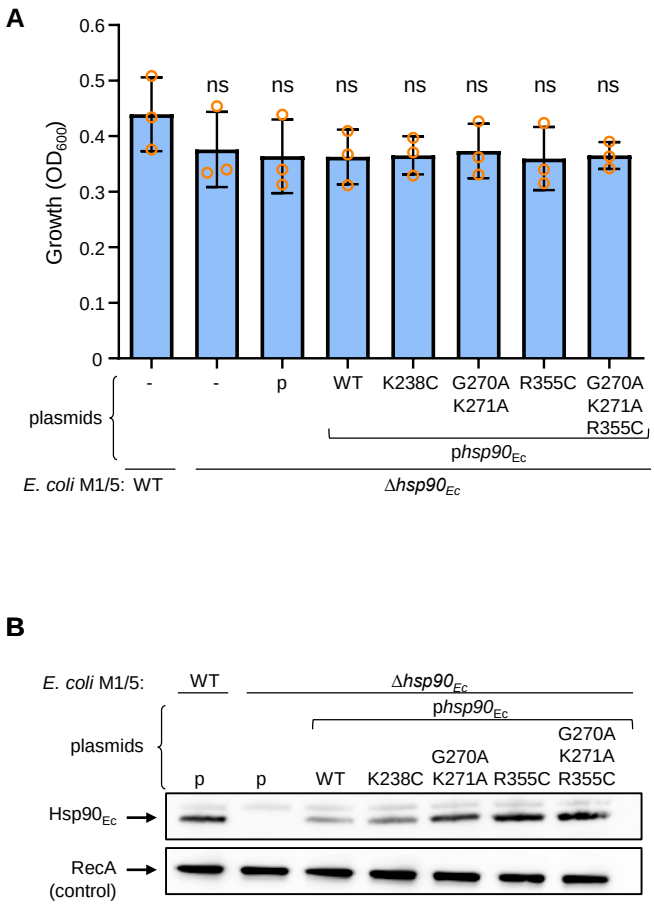

Fig. S10. Controls related to colibactin production in the presence of $Hsp90_{Ec}$ mutants.
(A) Bacterial growth is not affected by the presence of the mutants during the interaction with HeLa cells. Bacterial growth was determined 4 hours after exposition to human epithelial HeLa cells by measuring absorbance at 600 nm. Data from three replicates are shown as mean ± SD and results of one-way ANOVA tests indicate that the differences measured (vs WT) are not significant (ns, p-value > 0.05). (B) Control of the production of the $Hsp90_{Ec}$ mutants produced from the plasmids. Cultures of *E. coli* M1/5 and M1/5Δ*hsp90*$_{Ec}$ strains were grown without shaking in DMEM medium (Gibco) with 0.02 % arabinose. The samples were normalized and analyzed by Western blot. $Hsp90_{Ec}$ was detected using anti-Hsp90 antibody. Anti-RecA antibody was used as neutral loading control and shows that same amount of protein was loaded in the different wells.

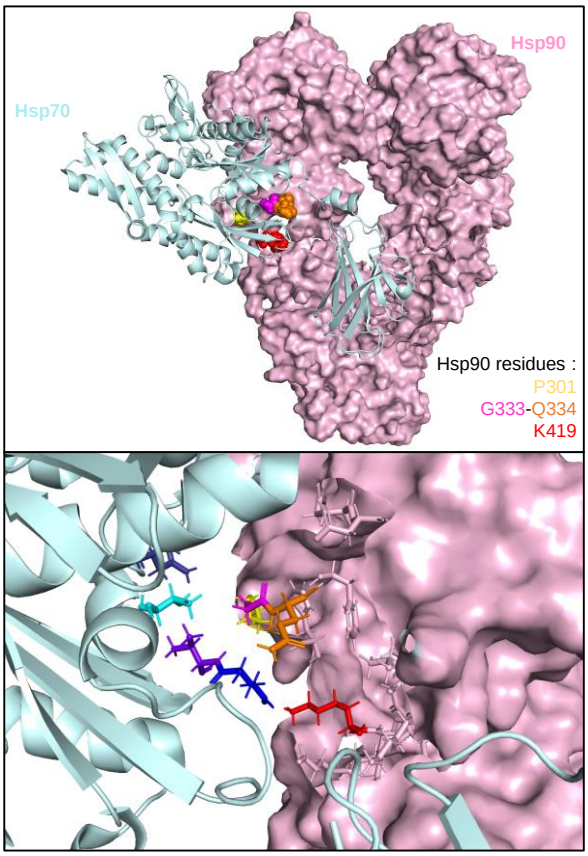

	Hsp90 residues		
Hsp90 (*S. oneidensis*)	K247	G279-K280	R364
Hsp90 (*E. coli*)	K238	G270-K271	R355
Hsp90α (Human)	P301	G333-Q334	K419
Hsp82 (*S. cerevisiae*)	P281	G313-Q314	K399
Grp94 (Human)	S347	G379-E380	K467

	Hsp70 residues	
DnaK (*S. oneidensis*)	N169-T172	E216-V217
DnaK (*E. coli*)	N170-T173	E217-V218
Hsp70 (Human)	N174-T177	E218-V219
Ssa1 (*S. cerevisiae*)	N112-T115	E155-V156
BiP (Human)	N200-T203	E243-V244

Fig. S11. Co-structure of eukaryotic Hsp90 and Hsp70 from Wang *et al.* (PDB : 7KW7) (22) **showing the homologous residues mutated in our study.** Hsp90 is represented in light pink surface structure, and Hsp70 in light cyan cartoon structure. Hsp90α (Human) residues important for interaction with Hsp70 (Human) are represented as spheres in the top image, and residues important for the interaction in both chaperones are represented as colored sticks in the bottom image. Homologous residues for Hsp90 and for Hsp70 are indicated in tables beside the structures. Some residues of Hsp90 and Hsp70 were hidden in the bottom image to better visualize the residues of interest. Note that this image only shows Hsp90 and Hsp70'C' (client loading) and does not show Hsp70'S' (scaffolding), co-chaperone and client. The images were prepared using PyMOL.

Table S1. Strains used in this study.

STRAINS	CHARACTERISTICS	SOURCE
***S. oneidensis* strains**		
MR1-R	*S. oneidensis* MR1 strain ATCC 700550, Rifampicine resistance.	(14)
MR1-R Δ*hsp90*$_{So}$	MR1-R with deletion of the *htpG* gene.	(12)
MR1-R *hsp90*$_{So}$(R364C)	MR1-R with mutations in *htpG* leading to the R364C substitution in Hsp90$_{So}$.	This study
MR1-R *hsp90*$_{So}$(G279A-K280A-R364C)	MR1-R with mutations in *htpG* leading to the G279A-K280A-R364C substitutions in Hsp90$_{So}$.	This study
MR1-R *dnaK*$_{So}$(E216A-V217A)	MR1-R with mutations in *dnaK* leading to the E216A-V217A substitutions in DnaK$_{So}$.	This study
***E. coli* strains**		
Bth101 Δ*hsp90*$_{Ec}$	*cya-99*, deleted of *htpG*.	(15)
MG1655 Δ*hsp90*$_{Ec}$	MG1655 strain deleted of *htpG*.	(13)
Bl21(DE3)	Used for protein overproduction. Codes for the T7 RNA polymerase.	Novagen
1047 /pRK2013	*E. coli "*helper" strain for conjugation.	(16)
CC118λpir	*λpir* lysogens of *E. coli* CC118. Used for pKNG101 plasmid replication.	(17)
M1/5	Wild-type *E. coli* strain; colibactin genotoxin producer.	(18)
M1/5 Δ*hsp90*$_{Ec}$	Deletion of the *htpG* gene in strain M1/5.	(19)
W3110	Wild-type *E. coli* strain.	Lab collection
W3110 Δ*dnaK dnaJ*	W3110 strain deleted of *dnaK* and *dnaJ*, Kanamycin resistance.	(4)

Table S2. Plasmids used in this study.

PLASMIDS	CHARACTERISTICS	SOURCE
Plasmids used for two-hybrid experiments		
pT18	pUT18C-linker vector. Carries the gene coding for the T18 adenylate cyclase domain of *B. pertussis*. IPTG inducible. Ampicillin resistance.	(20)
pT18-*dnaK*$_{So}$	pUT18C-linker plasmid carrying *dnaK*$_{So}$ gene.	This study
pT18-*hsp90*$_{So}$	pUT18C-linker plasmid carrying *hsp90*$_{So}$ gene.	(12)
pT25	pKT25-linker vector. Carries the gene coding T25 adenylate cyclase domain of *B. pertussis*. IPTG inducible. Kanamycin resistance.	(20)
pT25-*hsp90*$_{So}$	pKT25-linker plasmid carrying *htpG*$_{So}$ gene.	(12)
pT25-*hsp90*$_{So}$(K247C)	pKT25-linker plasmid carrying *htpG*$_{So}$ mutant leading to K247C substitution in Hsp90$_{So}$.	This study
pT25-*hsp90*$_{So}$(G279A-K280A)	pKT25-linker plasmid carrying *htpG*$_{So}$ mutant leading to G279A-K280A substitutions in Hsp90$_{So}$.	This study
pT25-*hsp90*$_{So}$(R364C)	pKT25-linker plasmid carrying *htpG*$_{So}$ mutant leading to R364C substitution in Hsp90$_{So}$.	This study
pT25-*hsp90*$_{So}$(G279A-K280A-R364C)	pKT25-linker plasmid carrying *htpG*$_{So}$ mutant leading to G279A-K280A-R364C substitutions in Hsp90$_{So}$.	This study
pT25-*dnaK*$_{So}$	pKT25-linker plasmid carrying *dnaK*$_{So}$ gene.	This study
pT25-*dnaK*$_{So}$(N169A-T172A)	pKT25-linker plasmid carrying *dnaK*$_{So}$ mutant leading to N169A-T172A substitutions in DnaK$_{So}$.	This study
pT25-*dnaK*$_{So}$(E216A-V217A)	pKT25-linker plasmid carrying *dnaK*$_{So}$ mutant leading to E216A-V217A substitutions in DnaK$_{So}$.	This study
Plasmids used for co-purification experiments		
pBad33-CBP	pBad33 plasmid carrying a sequence coding for a Calmodulin Binding Protein (CBP) tag. Arabinose inducible. Chloramphenicol resistance.	This study
pCBP-*hsp90*$_{So}$	pBad33 CBP plasmid carrying *htpG*$_{So}$ gene. Production of a fusion Hsp90 protein with a CBP tag at the N-terminal extremity.	This study

pCBP-*hsp90*$_{So}$(R364C)	pBad33 CBP plasmid carrying *htpG*$_{So}$ mutant leading to R364C substitution in Hsp90$_{So}$.	This study
pCBP-*hsp90*$_{So}$(G279A-K280A-R364C)	pBad33 CBP plasmid carrying *htpG*$_{So}$ mutant leading to G279A-K280A-R364C substitutions in Hsp90$_{So}$.	This study
pBad24	pBad24 plasmid. Arabinose inducible. Ampicillin resistance.	(9)
p*dnaK*$_{So}$-6His	pBad24 plasmid carrying the *dnaK*$_{So}$ gene with a sequence coding for a six-histidine (6His) tag. Production of DnaK$_{So}$ with a 6His tag at its C-terminal extremity.	This study
p*dnaK*$_{So}$(E216A-V217A)-6His	pBad24 plasmid carrying *dnaK*$_{So}$ mutant leading to E216A-V217A substitution in DnaK$_{So}$ and a 6His tag at its C-terminal extremity.	This study
pBad24-CBP	pBad24 plasmid carrying a sequence coding for a Calmodulin Binding Protein (CBP) tag. Arabinose inducible. Chloramphenicol resistance.	(10)
pCBP-*tilS*	pBad24 CBP plasmid carrying *tilS* gene from *S. oneidensis*. Production of a TilS protein fusion with a CBP tag at the N-terminal extremity.	(12)
Plasmids used for purifications		
pET*hsp90*$_{So}$	Plasmid allowing the production of Hsp90$_{So}$ wild-type.	(12)
pET*hsp90So*(R364C)	Plasmid allowing the production of Hsp90$_{So}$(R364C).	This study
pET*hsp90So*(G279A-K280A-R364C)	Plasmid allowing the production of Hsp90$_{So}$(G279A-K280A-R364C).	This study
Plasmids used for complementation experiments		
pBad33	pBad33 plasmid. Arabinose inducible. Chloramphenicol resistance.	(9)
p*hsp90*$_{So}$	pBad33 plasmid carrying *htpG*$_{So}$ gene.	(12)
p*hsp90*$_{So}$(K247C)	pBad33 plasmid carrying *htpG*$_{So}$ mutant leading to K247C substitution in Hsp90$_{So}$.	This study
p*hsp90*$_{So}$(G279A-K280A)	pBad33 plasmid carrying *htpG*$_{So}$ mutant leading to G279A-K280A substitutions in Hsp90$_{So}$.	This study
p*hsp90*$_{So}$(R364C)	pBad33 plasmid carrying *htpG*$_{So}$ mutant leading to R364C substitution in Hsp90$_{So}$.	This study
p*hsp90*$_{So}$(G279A-K280A-R364C)	pBad33 plasmid carrying *htpG*$_{So}$ mutant leading to G279A-K280A-R364C substitutions in Hsp90$_{So}$.	This study
p*hsp90*$_{So}$(W476R-L563A)	pBad33 plasmid carrying *htpG*$_{So}$ mutant leading to W476R-L563A substitutions in Hsp90$_{So}$.	(12)
p*hsp90*$_{Ec}$	pBad33 plasmid carrying *htpG*$_{Ec}$ gene.	This study

p*hsp90*$_{Ec}$(R355C)	pBad33 plasmid carrying *htpG*$_{Ec}$ mutant leading to R355C substitution in Hsp90$_{Ec}$.	This study
p*hsp90*$_{Ec}$(G270A-K271A-R355C)	pBad33 plasmid carrying *htpG*$_{Ec}$ mutant leading to G270A-K271A-R355C substitutions in Hsp90$_{So}$.	This study
p*dnaKdnaJ*$_{Ec}$	pBad33 plasmid carrying *dnaK*$_{Ec}$ and *dnaJ*$_{Ec}$ genes.	This study
p*dnaKdnaJ*$_{So}$	pBad33 plasmid carrying *dnaK*$_{So}$ and *dnaJ*$_{So}$ genes.	This study
p*dnaK(*E216A-V217A)*dnaJ*$_{So}$	pBad33 plasmid carrying *dnaK*$_{So}$ and *dnaJ*$_{So}$ with mutations on *dnaK*$_{So}$ leading to E216A-V217A substitutions in DnaK$_{So}$.	This study
Other plasmids		
p(AUA)*lacZ*	pBad33 plasmid carrying the construction ATG-4xATA-*lacZ* under the control of the pBad promoter.	(12)
p*lacZ*	pBad33 plasmid carrying *lacZ* gene under the control of the pBad promoter.	(12)
p*lacZ-tilS*$_{6His}$	pBad33 plasmid carrying *tilS* gene and a sequence coding for a six-histidine (6His) tag. Production of TilS with a 6His tag at its C-terminal extremity.	(12)
pKNG101	Suicide vector used for gene deletion and for mutagenesis. Carries the *sacB* cassette which causes sensitivity to sucrose, and a λ-pir-dependent origin of replication. Streptomycin resistance.	(21)

SI References

1. A. N. Kravats, *et al.*, Interaction of *E. coli* Hsp90 with DnaK Involves the DnaJ Binding Region of DnaK. *J. Mol. Biol.* **429**, 858–872 (2017).

2. H. Yang, *et al.*, Genome-scale metabolic network validation of *Shewanella oneidensis* using transposon insertion frequency analysis. *PLoS Comput. Biol.* **10**, e1003848 (2014).

3. A. Deutschbauer, *et al.*, Evidence-based annotation of gene function in *Shewanella oneidensis* MR-1 using genome-wide fitness profiling across 121 conditions. *PLoS Genet* **7**, e1002385 (2011).

4. P. Genevaux, *et al.*, *In vivo* analysis of the overlapping functions of DnaK and trigger factor. *EMBO Rep* **5**, 195–200 (2004).

5. J. C. Bardwell, E. A. Craig, Ancient heat shock gene is dispensable. *J. Bacteriol.* **170**, 2977–2983 (1988).

6. C. S. Gässler, *et al.*, Mutations in the DnaK chaperone affecting interaction with the DnaJ cochaperone. *Proc Natl Acad Sci U S A* **95**, 15229–15234 (1998).

7. C. Baraquet, L. Théraulaz, C. Iobbi-Nivol, V. Méjean, C. Jourlin-Castelli, Unexpected chemoreceptors mediate energy taxis towards electron acceptors in *Shewanella oneidensis*. *Molecular Microbiology* **73**, 278–290 (2009).

8. A. Battesti, E. Bouveret, The bacterial two-hybrid system based on adenylate cyclase reconstitution in *Escherichia coli*. *Methods* **58**, 325–334 (2012).

9. L. M. Guzman, D. Belin, M. J. Carson, J. Beckwith, Tight regulation, modulation, and high-level expression by vectors containing the arabinose PBAD promoter. *J. Bacteriol.* **177**, 4121–4130 (1995).

10. A. Battesti, E. Bouveret, Improvement of bacterial two-hybrid vectors for detection of fusion proteins and transfer to pBAD-tandem affinity purification, calmodulin binding peptide, or 6-histidine tag vectors. *Proteomics* **8**, 4768–4771 (2008).

11. O. Genest, J. R. Hoskins, J. L. Camberg, S. M. Doyle, S. Wickner, Heat shock protein 90 from *Escherichia coli* collaborates with the DnaK chaperone system in client protein remodeling. *Proc. Natl. Acad. Sci. U.S.A.* **108**, 8206–8211 (2011).

12. F. A. Honoré, V. Méjean, O. Genest, Hsp90 Is Essential under Heat Stress in the Bacterium *Shewanella oneidensis*. *Cell Rep* **19**, 680–687 (2017).

13. O. Genest, *et al.*, Uncovering a region of heat shock protein 90 important for client binding in *E. coli* and chaperone function in yeast. *Mol. Cell* **49**, 464–473 (2013).

14. C. Bordi, C. Iobbi-Nivol, V. Méjean, J.-C. Patte, Effects of ISSo2 insertions in structural and regulatory genes of the trimethylamine oxide reductase of *Shewanella oneidensis*. *J. Bacteriol.* **185**, 2042–2045 (2003).

15. O. Genest, J. R. Hoskins, A. N. Kravats, S. M. Doyle, S. Wickner, Hsp70 and Hsp90 of *E. coli* Directly Interact for Collaboration in Protein Remodeling. *J. Mol. Biol.* **427**, 3877–3889 (2015).

16. D. H. Figurski, D. R. Helinski, Replication of an origin-containing derivative of plasmid RK2 dependent on a plasmid function provided in trans. *Proc. Natl. Acad. Sci. U.S.A.* **76**, 1648–1652 (1979).

17. M. Herrero, V. de Lorenzo, K. N. Timmis, Transposon vectors containing non-antibiotic resistance selection markers for cloning and stable chromosomal insertion of foreign genes in gram-negative bacteria. *J. Bacteriol.* **172**, 6557–6567 (1990).

18. A. Wallenstein, *et al.*, ClbR Is the Key Transcriptional Activator of Colibactin Gene Expression in *Escherichia coli*. *mSphere* **5**, e00591-20 (2020).

19. C. Garcie, *et al.*, The Bacterial Stress-Responsive Hsp90 Chaperone (HtpG) Is Required for the Production of the Genotoxin Colibactin and the Siderophore Yersiniabactin in *Escherichia coli*. *J Infect Dis* **214**, 916–924 (2016).

20. D. Gully, E. Bouveret, A protein network for phospholipid synthesis uncovered by a variant of the tandem affinity purification method in *Escherichia coli*. *Proteomics* **6**, 282–293 (2006).

21. K. Kaniga, I. Delor, G. R. Cornelis, A wide-host-range suicide vector for improving reverse genetics in gram-negative bacteria: inactivation of the *blaA* gene of *Yersinia enterocolitica*. *Gene* **109**, 137–141 (1991).

22. R. Y.-R. Wang, *et al.*, Structure of Hsp90-Hsp70-Hop-GR reveals the Hsp90 client-loading mechanism. *Nature* **601**, 460–464 (2022).